

Multi-Product Supply Chain Optimization
for Energy Systems Semesterproject

presented by
Pielmaier, Konstantin
StudentID no. 24-935-835

Supervisor:
Gabriel Anselm Wiest, M.Sc.

Examiner: Prof. Dr.-Ing. André Bardow

Zürich, December 21, 2025

Abstract

This work integrates a spatio-temporal multi-product supply chain framework into the energy system model EnergyScope to study stakeholder participation, demand elasticity, and price formation in multi-sector energy systems. EnergyScope, formulated as a central planner minimizing total system cost under fixed demand, is reformulated as a coordinated market cleared by an independent system operator maximizing social welfare. Resources, conversion technologies, storage, and demands are represented as profit-seeking stakeholders interacting through supply and demand bids. Consumer flexibility is introduced by a piecewise linear approximation of an elastic demand curve, transforming the optimization problem from a linear to a quadratic program while preserving computational efficiency.

When demand is fixed, linear market clearing becomes equivalent to the central planner outcome. Stakeholder responses to price signals emerge only when demand is elastic. A case study of Germany's multi-sector energy system in 2050 shows how demand elasticity changes investment and operation decisions that shape prices. Market prices correspond to the shadow prices of nodal balance constraints and are set by the marginal plant or storage unit. Flexible consumers reduce zero-price hours during high renewable generation, limit price-peaks during scarcity, and stabilize prices in systems with high shares of renewables.

In coordinated market models, elastic demand is required to capture stakeholder interactions. Integrating this into EnergyScope provides a feasible and consistent foundation for analyzing investment, operation, and endogenous price formation in highly decarbonized and integrated future energy systems.

Keywords: energy system modeling; supply chain; demand elasticity; price formation

Contents

Abstract	ii
List of Acronyms	v
List of Figures	vi
List of Tables	viii
1. Introduction	1
2. Method	3
2.1. Multi-product Supply Chain	3
2.1.1. Coordinated market clearing problem	4
2.1.2. Economic properties	6
2.1.3. Spatio-temporal graph	7
2.2. Price formation	8
3. Modeling	9
3.1. EnergyScope	9
3.2. Spatio-temporal graph	10
3.3. Stakeholders	11
3.4. Product balance	12
3.5. Supply bids	13
3.6. Demand bids	14
3.6.1. Demand curves	14
3.6.2. Fixed demand	15
3.6.3. Perfectly inelastic demand up to VOLL	15
3.6.4. Linear demand	16
3.6.5. Log-log demand	16
3.6.6. Piecewise linear demand	16

Contents

3.7. Objective function	20
3.7.1. Total cost	20
3.7.2. Social welfare	21
4. Case Study	22
4.1. Data	22
4.2. Price scenarios	22
4.3. Demand elasticity	24
4.4. Electricity Prices	30
4.4.1. Dependence on Emission Cap	30
4.4.2. Daily profile of electricity prices	31
4.4.3. Zero- and peak-price hours	37
5. Conclusion and Outlook	39
Bibliography	41
A. Sets, Parameters, and Variables	45
A.1. Sets and Indices	45
A.2. Parameters	46
A.2.1. Time Parameters	46
A.2.2. Technology Parameters	46
A.2.3. Cost Parameters	46
A.2.4. Demand Parameters	46
A.2.5. Piecewise Linear Demand Parameters	47
A.3. Decision Variables	47
A.3.1. Independent Variables	47
A.3.2. Dependent Variables	47
A.3.3. Dual Variables	48
A.4. Objective Variables	48
B. Flows	49

List of Acronyms

DAG directed acyclic graph. 6

GWP global warming potential. 25, 26, 37, 38

ISO independent system operator. 1, 4, 6

LP linear program. 1, 5, 7, 9, 20, 21

MC marginal costs. 4, 8, 13, 29, 32, 34, 37, 38

MSV marginal storage value. 8, 13, 34

O&M operation and maintenance. 13, 20, 21, 46, 47

PV photovoltaic. 22, 31, 35

PWL piecewise linear. 2, 14, 16–19, 21, 25, 45

QP quadratic program. 21, 25

SC supply chain. 1–17, 20–22, 25, 30, 40, 45

SoC state-of-charge. 12, 34

TD typical day. 1, 10, 12, 29, 31, 32, 34, 35

VOLL value-of-lost-load. 2, 6, 14–16, 18, 19, 29

VRE variable renewable energy. 8

WTP willingness to pay. 4, 15, 27

List of Figures

2.1.	Node (left), stakeholder (center), and product (right) representation of SC.	3
2.2.	Illustration of the coordinated market.	4
2.3.	Primal and dual coordinated market clearing problems.	5
2.4.	Spatio-temporal graph.	7
2.5.	Hourly demand and supply curve intersection.	8
3.1.	EnergyScope.	9
3.2.	Typical days.	10
3.3.	Set structure.	11
3.4.	Demand curves.	14
3.5.	Electricity demand curve zoomed in around the reference point.	18
3.6.	Elasticity along PWL demand curve.	19
3.7.	Market situation in the multi-product SC EnergyScope model.	20
3.8.	Illustration of quadratic PWL consumer term in the objective function.	21
4.1.	Capacity factor heat map for PV.	23
4.2.	Capacity factor heat map for onshore wind.	23
4.3.	Demand curves with different elasticities for the normal-price scenario.	24
4.4.	Solve time versus GWP for the normal-price scenario.	25
4.5.	Normalized social welfare versus GWP for normal-price scenario.	26
4.6.	Total system cost versus GWP for high- and low-price scenarios.	27
4.7.	Electricity demand curve for the low-price scenario in hour 19 of TD 8.	28
4.8.	Electricity demand curve for the high-price scenario in hour 1 of TD 6.	28
4.9.	Yearly average electricity price versus GWP for the normal-price scenario.	30
4.10.	Hourly electricity price averaged over all TDs for the normal-price zero-emission scenario.	31
4.11.	Hourly electricity price on TD 3 for the normal-price zero-emission scenario.	32
4.12.	Stakeholder flow on TD 3 for the normal-price zero-emission scenario.	33
4.13.	Hourly electricity price on TD 9 for the normal-price zero-emission scenario.	34

List of Figures

4.14. Hourly charging, discharging, and SoC of lithium-ion battery on TD 9 for the normal-price zero-emission scenario with 5 % elasticity.	35
4.15. Hourly electricity price on TD 4 for the normal-price zero-emission scenario.	36
4.16. Hourly electricity price on TD 11 for the normal-price zero-emission scenario.	36
4.17. Number of zero-price hours per year versus GWP in the normal-price scenario.	37
4.18. Share of renewable energy supply in the normal-price scenario.	38
4.19. Number of peak-price hours per year versus GWP in the normal-price scenario.	38
 B.1. Stakeholder flow on TD 9 for the normal-price zero-emission scenario.	49
B.2. Stakeholder flow with fixed demand on TD 4 for the normal-price zero-emission scenario.	50
B.3. Stakeholder flow with 5% elasticity on TD 4 for the normal-price zero-emission scenario.	51
B.4. Stakeholder flow with fixed demand on TD 11 for the normal-price zero-emission scenario.	52
B.5. Stakeholder flow with 5% elasticity on TD 11 for the normal-price zero-emission scenario.	53

List of Tables

4.1. Yearly average end-use prices for low-, normal-, and high-price scenarios. . .	24
---	----

1. Introduction

The transition toward affordable, clean, and secure energy systems relies on fast expansion of renewable generation together with widespread electrification of heating and mobility. The intermittency of renewable resources, the resulting need for energy storage, and increased multi-sector coupling raise system complexity. To support long-term planning, energy system models based on optimization are widely used, which are typically formulated as large-scale linear programs (LPs). An example is EnergyScope developed by Limpens et al. [1], an open-source model that optimizes investment and operation of national or regional multi-energy systems using representative typical days (TDs).

In most energy system models such as EnergyScope, demand is fixed and must be supplied at minimum total system cost. This implicitly assumes a central planner who dictates resource allocation across all assets [2]. While this identifies cost-optimal technology choices on the supply side, it does not reflect how modern energy systems operate. In practice, decentralized stakeholders such as producers, storage operators, and consumers own assets, interact through markets, and seek to maximize profit by responding to price signals [3].

To overcome the central planner assumption, energy systems can instead be modeled using coordinated markets. In these formulations, stakeholders submit bids to an independent system operator (ISO), who clears the market to maximize social welfare subject to generation and transmission constraints [2]. This process ensures reliable energy supply to consumers while providing transparent prices that reflect the underlying value of energy [3]. Yang Shu et al. [4] compared central planner and market equilibrium formulations at the national scale and found that considering competing stakeholders can significantly change energy system outcomes.

Tominac et al. [2, 3] introduce a spatio-temporal multi-product supply chain (SC) framework that formulates coordinated markets as optimization problems. The framework links physical resource allocation in the primal problem with market price formation through the dual variables of nodal balance constraints. The resulting solution corresponds to a competitive equilibrium in which stakeholders recover their costs and can earn profits.

1. Introduction

More broadly, market models can be classified as partial or general equilibria. General equilibrium models cover all markets in an economy but rely on aggregation that limits technological and temporal detail for energy system applications [5, 6]. The multi-product SC framework is a partial equilibrium model that endogenizes a subset of coupled markets.

This semester project investigates the feasibility and usefulness of integrating a coordinated market formulation into a long-term energy system model. Specifically, it explores the integration of the spatio-temporal multi-product SC optimization framework into EnergyScope. While EnergyScope enforces fixed demand, coordinated market formulations rely on voluntary stakeholder participation driven by economic incentives. Imposing demand destroys key economic properties of the market clearing formulation [2], motivating an alternative demand representation compatible with market equilibrium optimization and endogenous price formation. Against this background, the work addresses the following research questions:

1. Can the spatio-temporal multi-product SC framework be integrated into EnergyScope, while preserving computational efficiency for long-term energy system planning?
2. How should consumer demand be modeled in this integrated framework, given that imposed demand destroys the key economic properties of coordinated market?
3. What additional insights does a market equilibrium provide compared to a central planner, particularly with respect to endogenous price formation?

To answer these questions, EnergyScope is reformulated as a coordinated market using the spatio-temporal multi-product SC framework. Instead of enforcing demand satisfaction, consumers are modeled as price-responsive stakeholders. Several demand representations are examined, ranging from the value-of-lost-load (VOLL) to a piecewise linear (PWL) approximation of an elastic log–log demand curve. This allows demand to respond to prices while preserving the computational efficiency of the optimization for large-scale energy system analysis. The framework is applied to a case study of Germany’s coupled electricity and heating system in 2050, together with a sensitivity analysis on demand elasticity.

The report is structured as follows. Chapter 2 introduces the multi-product SC framework, its interpretation as a coordinated market, and its spatio-temporal extension. Chapter 3 describes its integration into EnergyScope, including the spatio-temporal graph, stakeholder representation, demand modeling, and the formulation of product balances and the social welfare objective. Chapter 4 presents the results of the German case study, focusing on system outcomes, stakeholder participation, and price formation under varying demand elasticities. Chapter 5 concludes and briefly outlines directions for future research.

2. Method

This chapter introduces the multi-product SC framework proposed by Tominac et al. [2]. The optimization problem is formulated as a coordinated market clearing problem that allocates resources to stakeholders and determines market prices. We summarize the market formulation and the key derived economic properties to enable adaptation to EnergyScope in the subsequent chapter.

2.1. Multi-product Supply Chain

In SC optimization, suppliers $i \in S$ inject input products $p \in P$ into the SC, which processors $t \in T$ convert into more valuable output products to satisfy the demand of consumers $j \in D$. Transporters $l \in L$ connect stakeholders by enabling product flows between nodes $n \in N$. As shown in Figure 2.1, the SC can be represented as a node, stakeholder, or product graph [2].

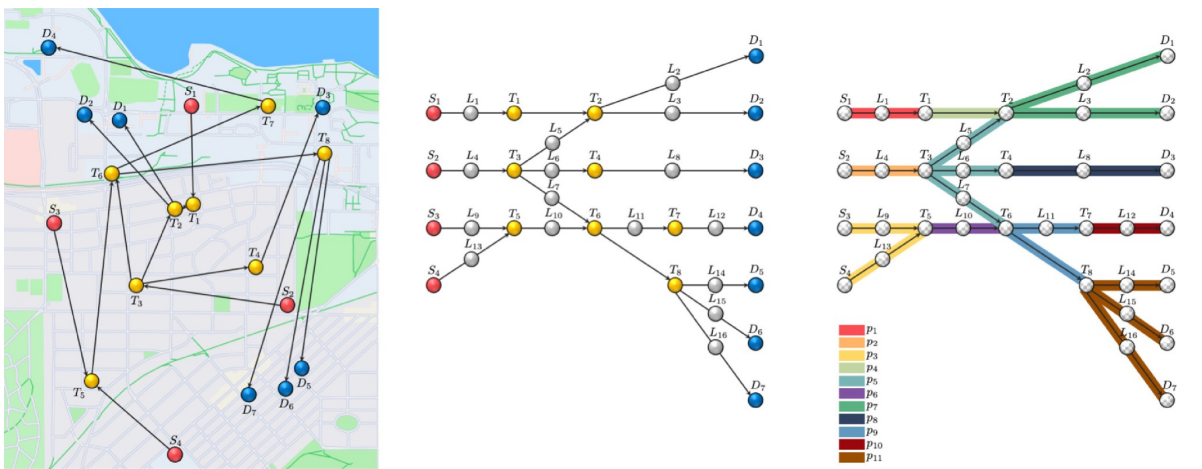


Figure 2.1.: Node (left), stakeholder (center), and product (right) representation of SC [2].

2. Method

2.1.1. Coordinated market clearing problem

In contrast to a central planner, who controls all assets to minimize total system cost, the multi-product SC is formulated as a coordinated market [2]. Independent stakeholders own assets and seek to maximize their individual profits ϕ , as illustrated in Figure 2.2. The mathematical formulation of the market clearing optimization is shown in Figure 2.3.

Stakeholders participate in the coordinated market by submitting bids to the ISO, specifying both bid capacities $\bar{d}, \bar{s}, \bar{f}, \bar{\xi}$ and values α . On the producer side, suppliers, processors, and transport providers bid their marginal costs (MC) to provide services, while consumers bid their willingness to pay (WTP) to receive products. Based on this bidding information, the ISO solves the primal market clearing problem with the objective of maximizing social welfare. The ISO allocates the resulting physical product flows s, d, f, ξ back to stakeholders, subject to nodal product balance constraints. Product conversion by processors is captured linearly through reference products and relative yield coefficients γ . Unless consumer bids are sufficient to remunerate all upstream services in the SC required to provide a product, the market for that product runs dry [2].

In addition to the primal problem, the ISO implicitly solves the dual market clearing problem. The dual variables of the nodal product balance constraints, also referred to as clearing constraints, are the nodal market clearing prices π , while the duals of the capacity constraints are the marginal capacity prices $\bar{\lambda}$. In the dual problem, the ISO minimizes capacity margins while preserving the economic driving forces of the market [2].

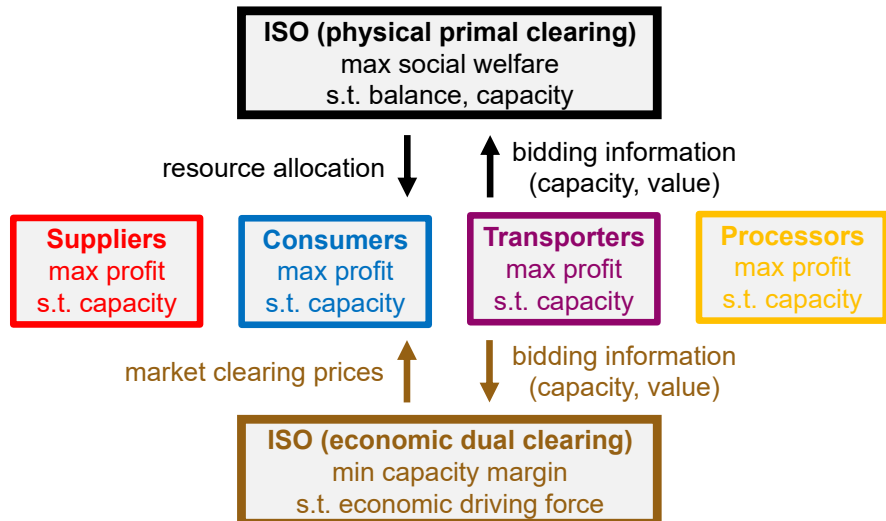


Figure 2.2.: Illustration of the coordinated market.

2. Method

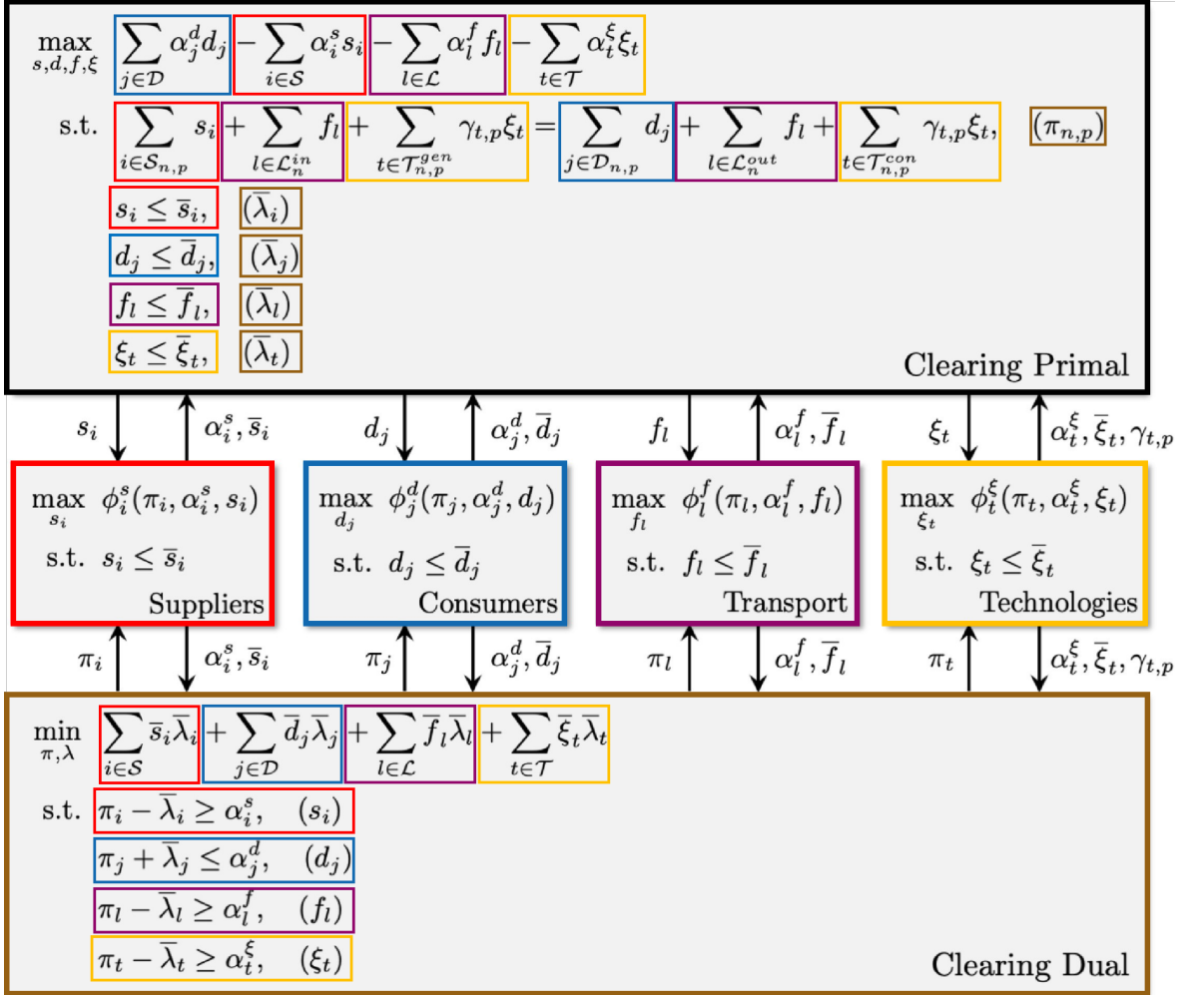


Figure 2.3.: Primal and dual coordinated market clearing problems [2].

To maximize social welfare, the coordinated market prioritizes high bids from consumers and low bids from suppliers, processors, and transporters. For suppliers, when the market price exceeds the bid value, the accepted bid costs α_s . The supplier is remunerated π_s and earns a profit of $(\pi - \alpha)s$. The same logic applies to processors and transporters. On the demand side, consumer bids are accepted when the market price is below the bid value, in which case the profit is $(\alpha - \pi)d$ [2].

Market resolution approaches based on game theory, such as Bertrand or Cournot competition, are explicit in price and quantity and therefore nonlinear [7]. Similarly, direct contract negotiation approaches, such as Stackelberg leader–follower relationships, are typically bilevel and nonlinear [8]. In contrast, the coordinated market auction of the multi-product SC determines clearing prices via dual shadow prices and is formulated as a LP [2].

2. Method

2.1.2. Economic properties

Sampat et al. [9] establish key economic properties of the coordinated market clearing formulation. The most relevant properties for adapting the multi-product SC framework to EnergyScope are summarized below.

1. The coordinated market maximizes collective profits while guaranteeing nonnegative individual profits. Every stakeholder recovers its costs and does not lose money.
2. The optimal solution corresponds to a competitive equilibrium.
3. Market clearing prices are bounded by stakeholder bids.
4. Revenue adequacy holds, meaning that payments collected from consumers are sufficient to cover payments to suppliers, processors, and transport providers. Since the ISO can also collect revenue from negative consumer and supplier bids, the formulation remains consistent under negative prices.
5. With nonnegative transport bids, no inefficient transportation cycles are allocated.

The coordinated market relies on voluntary stakeholder participation driven by economic incentives. The ISO does not assume participation by any stakeholder. Tominac et al. [2] show that forcing stakeholder participation by imposing demand destroys key economic properties. While stakeholders continue to seek profits and revenue adequacy still holds, price boundedness is lost, meaning stakeholders can lose money. The resulting market outcome is no longer a competitive equilibrium, and inefficient services, such as transportation cycles, may be allocated. Forcing the participation of even a single stakeholder can propagate inefficiencies throughout the SC.

Instead, Tominac et al. [2] advocate for market participation driven by economic incentives. Market-activating bids represent break-even bid values that clear the market with zero profit and define threshold clearing prices for market existence. An example is the VOLL during scarcity events in electricity markets. Furthermore, Tominac et al. [2] show that market-activating bids can be calculated from the topology of the product-based stakeholder graph shown in Figure 2.1, which typically forms a directed acyclic graph (DAG). In energy system optimization, this perspective may provide insight into merit order formation and the emergence of endogenous market prices. Such understanding could support policymakers by informing whether market activation, for example for hydrogen, requires market entry as a stakeholder or providing incentives that shift stakeholder bids.

2. Method

2.1.3. Spatio-temporal graph

To remunerate load-shifting flexibility from data centers, Zhang and Zavala [10] introduce space-time flows in an electricity market clearing formulation. Tominac et al. [3] generalize these space-time flows to the multi-product SC optimization framework.

As shown in Figure 2.4, steady-state snapshots of the multi-product SC are connected over time to make the SC dynamic. Spatial nodes $n \in N$ combined with time steps $t \in T$ become space-time nodes $s = (n, t) \in S$, which define a spatio-temporal graph over the planning horizon. Suppliers, processors, and consumers are located at space-time nodes, while transporters and storage are associated with arcs $a \in A$ that connect these nodes. Thereby, the extended multi-product SC is able to capture spatial transport, storage interpreted as temporal transport, and time delays [3].

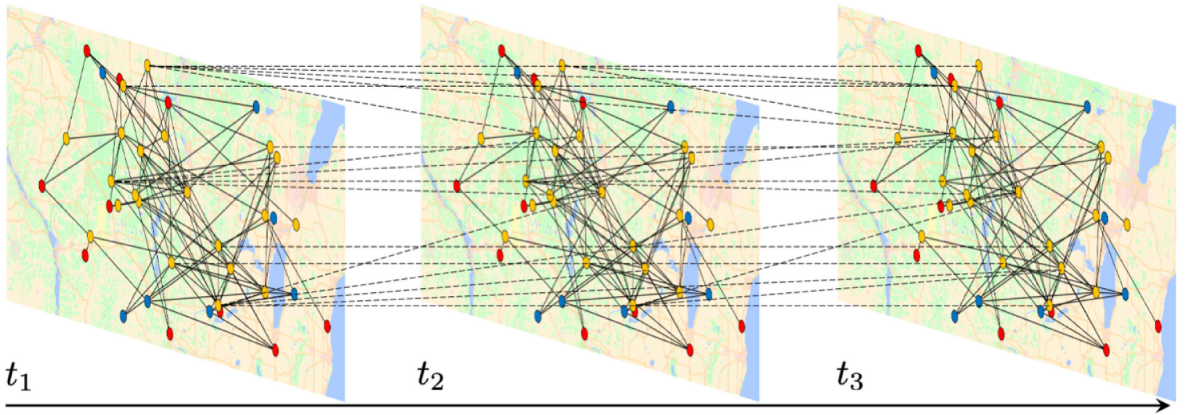


Figure 2.4.: Spatio-temporal graph [3].

Tominac et al. [3] show that the key economic properties of the coordinated market, including cost recovery, competitive equilibrium, price boundedness, revenue adequacy, and efficiency, are preserved in the spatio-temporal extension. They also establish temporal properties, showing that the optimal objective value of the dynamic SC is greater than or equal to that of the combined steady-state SCs, as intertemporal coupling adds flexibility.

Spatio-temporal prices emerge from the clearing constraints enforced at each space-time node. These prices allow revenue streams to flow both forward and backward in time, enabling transport and storage to mitigate spatio-temporal price volatility, as demonstrated in the waste-to-energy case study by Tominac et al. [3]. Simplified examples in the supplementary material are used to validate the initial implementation of the spatio-temporal multi-product SC optimization framework formulated as a LP.

2.2. Price formation

Tominac et al. [3] further establish that only stakeholders allocated their full capacity can earn positive profits. All other stakeholders either do not participate or operate at the margin. Marginal plants set the market price. Their revenues therefore equal their costs, resulting in zero profit. Consequently, the mathematical shadow prices of the multi-product SC optimization can also be interpreted as the MC of the marginal plant.

Brown et al. [11] investigate price formation in systems with demand elasticity and storage bidding, despite high shares of zero MC variable renewable energy (VRE). Price formation is illustrated using the hourly intersection of supply and demand curves shown in Figure 2.5. On the one hand, **when VRE exceeds both demand and storage charging capacity**, VRE is marginal. **When VRE exceeds demand but not storage charging capacity**, storage charging is marginal. On the other hand, **when demand exceeds both VRE and storage discharging capacity**, demand is marginal. **When demand exceeds VRE but not storage discharging capacity**, storage discharging is marginal. Prices are zero if VRE is marginal and non-zero if demand or storage is marginal. Storage bids are non-zero due to the marginal storage value (MSV). This value reflects the storage unit's opportunity cost and arises from scarcity pricing during periods when demand is marginal.

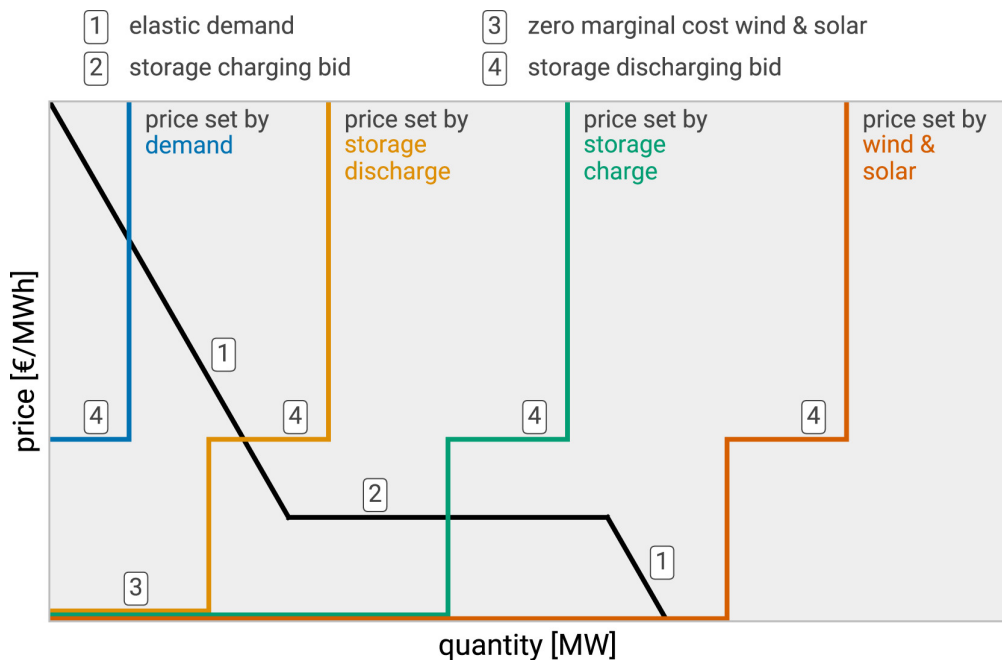


Figure 2.5.: Hourly demand and supply curve intersection [11].

3. Modeling

This chapter presents the multi-product SC EnergyScope model, derived from the integration of EnergyScope, developed by Limpens et al. [1], with the multi-product SC optimization framework proposed by Tominac et al. [2]. After a brief introduction to EnergyScope, the chapter focuses on the modifications required for the multi-product SC formulation. The sets, parameters, and variables of the integrated model are listed in Appendix A.

3.1. EnergyScope

EnergyScope is an open-source energy system model, illustrated in Figure 3.1, that optimizes the long-term investment and operation of national or regional energy systems. Formulated as LP, it minimizes total system cost while accounting for technological and environmental constraints. Comprehensive documentation of the core version is available online [12].

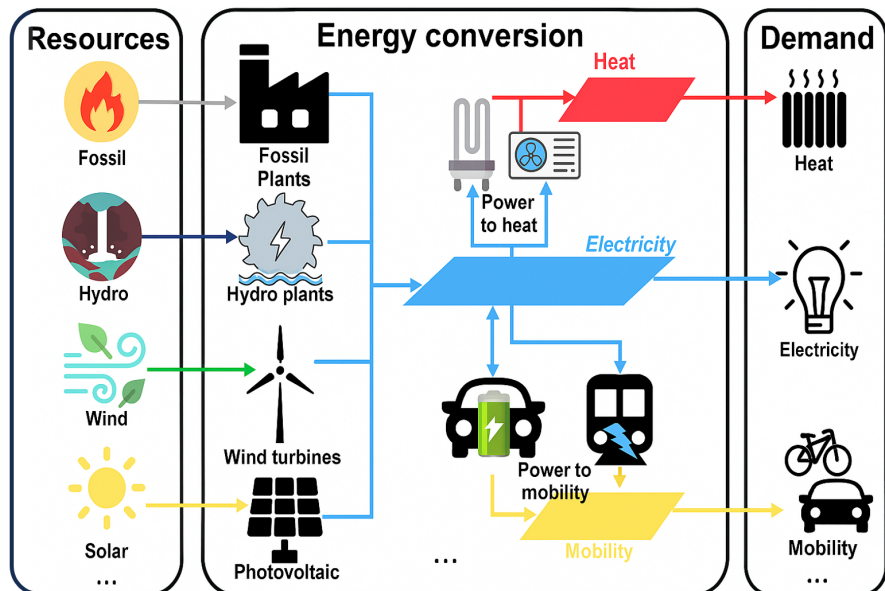


Figure 3.1.: EnergyScope [1].

3.2. Spatio-temporal graph

As discussed in Section 2.1.3, the multi-product SC is formulated on a spatio-temporal graph. Since the core EnergyScope model approximates an entire country with a single node, the spatial dimension simplifies to one national node $n \in N$.

EnergyScope clusters the 8,760 hourly periods of a year into a set of hourly resolved TDs using the algorithm proposed by Domínguez et al. [13]. This selection of representative days reduces computational complexity while preserving the accuracy of the energy system [1]. A detailed description of the TD methodology, together with a Python script to generate TDs, is available online [14]. Consistent with EnergyScope, we extend the temporal dimension of the spatio-temporal graph to explicitly include both hours $h \in H$ and TDs $td \in TD$.

As illustrated in Figure 3.2, storage introduces intertemporal coupling so that the time steps of duration t_{op} [h] cannot be treated independently. Whereas daily storage follows the same hourly sequence within each TD, seasonal storage requires the full annual chronology, which is reconstructed using the method of Gabrielli et al. [15]. Each combination of hour and TD is mapped to a period $t \in T$, with parameter w [-] denoting the yearly cardinality.

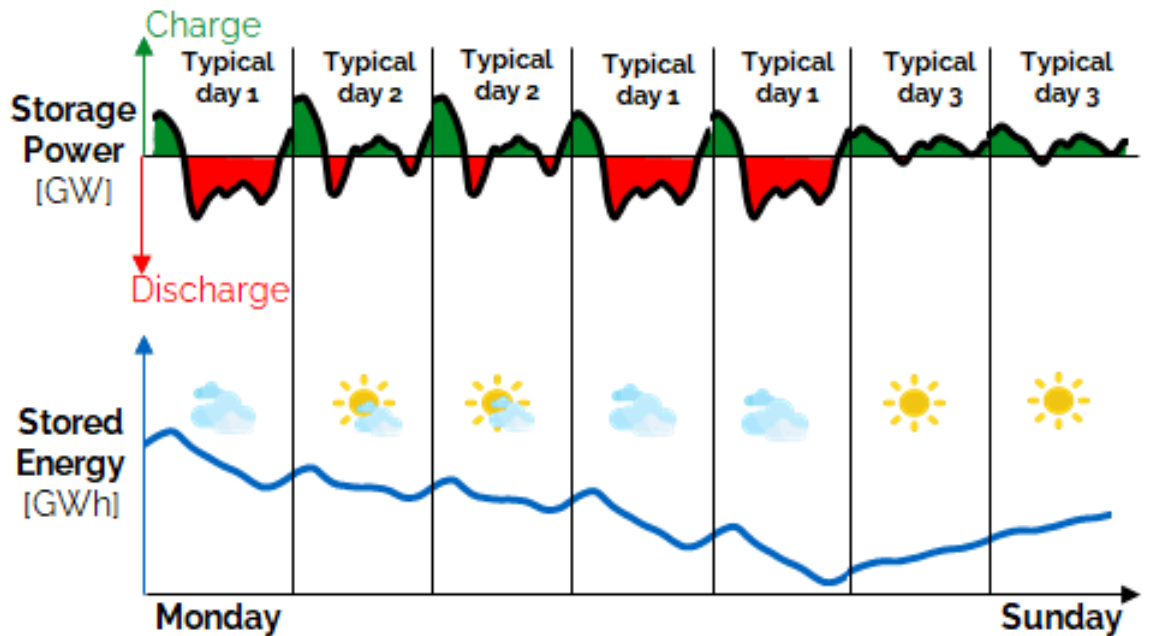


Figure 3.2.: Typical days [1].

3. Modeling

3.3. Stakeholders

As illustrated in Figure 3.1 [1], the core EnergyScope model is structured around resources $i \in RES$, technologies $j \in TECH$, and demands of end-use type $eut \in EUT$. The following set interface maps this structure to the stakeholders of the multi-product SC framework introduced in Section 2.1.

The multi-product SC EnergyScope model distinguishes five **stakeholder types**. **Suppliers** $s \in S \subseteq RES$ correspond to resources and inject products into the SC. **Processors** $p \in P \subset TECH$ correspond to conversion technologies that transform input products into output products. **Storage** stakeholders $sto \in STO \subset TECH$ correspond to storage technologies that enable the transfer of products between temporal nodes. **Transporters** correspond to infrastructure $inf \in INF \subset TECH$ for product transport between spatial nodes. However, for a single node system they are disabled, while associated infrastructure costs, such as grid expansion, are still accounted for. **Consumers** $c \in C \subseteq EUT$ correspond to end-use types and withdraw end-use demand. Figure 3.3 shows the EnergyScope sets remaining for the electricity and heating case study in Chapter 4. The interface allows straightforward integration of additional sectors such as mobility.

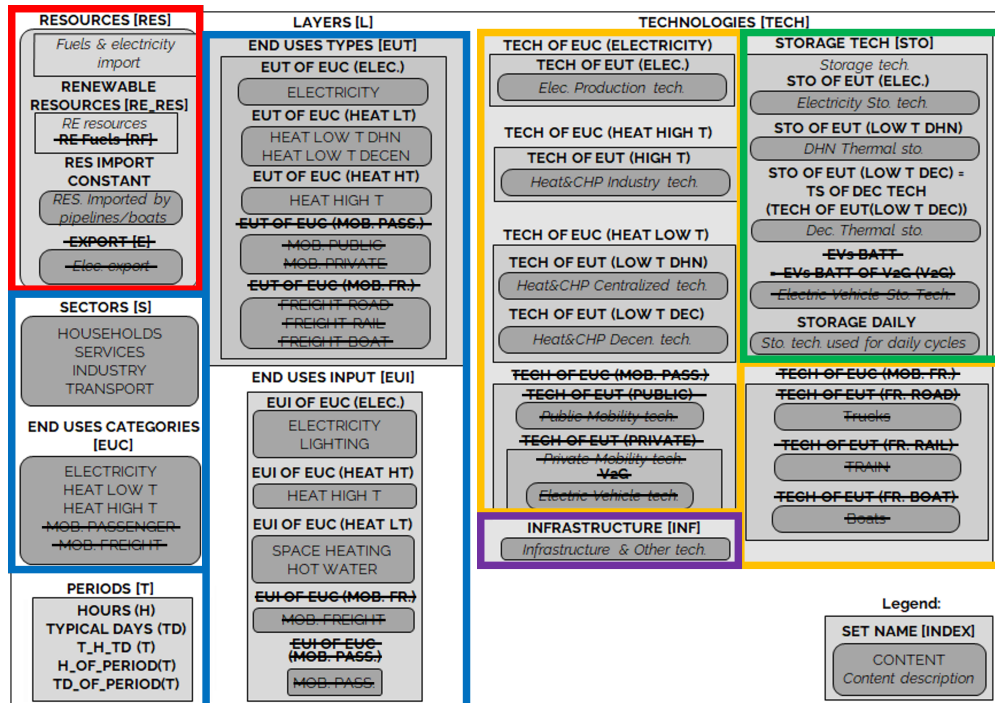


Figure 3.3.: Set structure [1].

3. Modeling

Each stakeholder has an independent flow variable. For **suppliers**, this is the supply variable g [GW], for **processors** the conversion variable e [GW], and for **consumers** the demand variable d [GW]. In the single node system, the **transporter** flow variable and its associated constraints are disabled. **Storage** requires the two independent charging $\text{Storage}_{\text{in}}$ [GW] and discharging $\text{Storage}_{\text{out}}$ [GW] power flow variables. Due to the storage balance equations, the storage state-of-charge (SoC) $\text{Storage}_{\text{level}}$ [GWh], defined over all periods for seasonal storage, and $\text{Storage}_{\text{level,daily}}$ [GWh], defined over all hour and TD combinations for daily storage $sto_{\text{daily}} \in STO_{\text{daily}} \subset TECH$, are dependent variables.

In the core EnergyScope model, the technology operation variable acts as the SoC for daily storage. In contrast, in the multi-product SC stakeholder formulation, storage SoC is treated separately from processor flow, which necessitates the additional $\text{Storage}_{\text{level,daily}}$ variable to enforce the daily storage consistency constraint given in Equation 3.1.

$$\text{Storage}_{\text{level}}^{j,n,t} = \text{Storage}_{\text{level,daily}}^{j,n,h,td} \quad \forall j \in STO_{\text{daily}}, n, t, h[t], td[t] \quad (3.1)$$

3.4. Product balance

The products of the multi-product SC correspond to the layers $l \in L = RES \cup EUT$ of EnergyScope, which comprise all resources and end-use types. These products represent the energy carriers exchanged among stakeholders across the spatio-temporal graph.

Rather than adopting the reference products and yields of the multi-product SC framework, we retain the EnergyScope conversion structure through the parameter $\text{layers}_{\text{in,out}}^{[-]}$, which assigns products to suppliers and implements the conversion efficiencies of processors. This leads to the multi-product SC EnergyScope nodal balance in Equation 3.2.

$$\begin{aligned} & \sum_s \text{layers}_{\text{in,out}}^{s,l} \cdot g^{s,n,h,td} + \sum_p^{\text{layers}_{\text{in,out}}^{p,l} > 0} \text{layers}_{\text{in,out}}^{p,l} \cdot e^{p,n,h,td} + \sum_{sto} \text{Storage}_{\text{out}}^{sto,l,n,h,td} \\ &= \sum_c^{\text{c}=l} d^{c,n,h,td} - \sum_p^{\text{layers}_{\text{in,out}}^{p,l} < 0} \text{layers}_{\text{in,out}}^{p,l} \cdot e^{p,n,h,td} + \sum_{sto} \text{Storage}_{\text{in}}^{sto,l,n,h,td} \end{aligned} \quad (3.2)$$

$\forall l, n, h, td$

3.5. Supply bids

In the multi-product SC framework, stakeholders participate in the market clearing through bid capacities and values. Bid capacities reflect resource availability as well as technological capacity factor and size constraints. Bid values derive from the MC at which stakeholders can provide their service.

In general, the MC of power plants consist of fuel costs c_{fuel} , carbon costs c_{CO_2} , and other variable operation and maintenance (O&M) costs c_{var} , as expressed in Equation 3.3.

$$\text{MC} = c_{\text{fuel}} + c_{\text{CO}_2} + c_{\text{var}}. \quad (3.3)$$

EnergyScope captures the MC of technologies through fuel costs, while carbon costs and variable O&M costs are neglected. Because fuels enter the multi-product SC as resources, supplier bid values correspond to the operational resource costs c_{op} [$\text{M}\epsilon \text{GWh}^{-1}$]. To remain consistent with EnergyScope and avoid double counting, no additional bid values are assigned to processors. Storage and transport technologies likewise do not carry explicit bid values. As described by Brown et al. [16], storage technologies bid implicitly through their MSV, which reflects the intertemporal arbitrage value of stored energy together with efficiency losses governed by the storage balance constraint. Transporter bids only become relevant with multiple nodes. Although currently neglected, future work could investigate carbon or variable O&M costs as processor bid values and explicit storage bidding.

As stakeholder bids reflect short-run MC (SRMC) rather than long-run MC (LRMC), investment costs c_{inv} [$\text{M}\epsilon \text{GW}^{-1}$] and fixed O&M costs c_{maint} [$\text{M}\epsilon \text{GW}^{-1} \text{a}^{-1}$] are excluded from the bid values. Instead, these fixed technology costs are scaled with the installed capacity F [GW, storage GWh], as given by Equations 3.4 and 3.5, and directly accounted for in the objective function to optimize investment decisions.

$$C_{\text{inv}}^j = c_{\text{maint}}^j \cdot F^j \quad \forall j \quad (3.4)$$

$$C_{\text{maint}}^j = c_{\text{maint}}^j \cdot F^j \quad \forall j \quad (3.5)$$

3.6. Demand bids

In EnergyScope, demand is fixed and must be fully met by supply. However, as shown by Tominac et al. [2], forcing stakeholder participation destroys key economic properties of the coordinated market clearing formulation. In particular, under fixed consumer demand, it can no longer be guaranteed that all stakeholders remain profitable. This tension between EnergyScope and the multi-product SC framework motivates the extended discussion in this section on how consumer demand should be represented within the combined model.

3.6.1. Demand curves

Brown et al. [11] analyze several demand curves, illustrated in Figure 3.4, including perfectly inelastic demand, perfectly inelastic demand up to the VOLL, linear demand, and a PWL approximation of a log–log demand curve. Nonlinear demand curves are not considered, because they lead to an objective function of higher order than quadratic, which increases the computational complexity of the optimization problem.

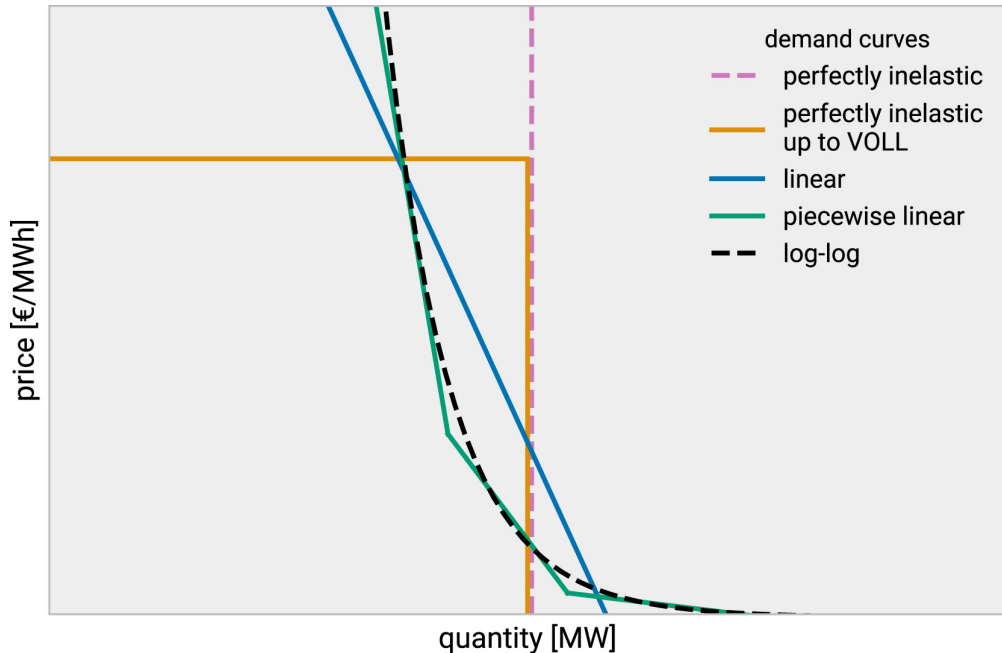


Figure 3.4.: Demand curves [11].

3.6.2. Fixed demand

Perfectly inelastic demand corresponds to the fixed demand of EnergyScope. The EnergyScope end-use demands $\text{End}_{\text{uses}}^{\text{c}, \text{h}, \text{td}}$ [GW] define the reference demand $d_{\text{ref}}^{\text{c}, \text{h}, \text{td}}$ [GW] of the corresponding consumer in the multi-product SC, as shown in Equation 3.6. Perfectly inelastic demand implies an infinite consumer WTP up to the reference demand and zero WTP beyond it. In the multi-product SC EnergyScope model, this is enforced by setting each consumer's flow variable equal to its reference demand via Constraint 3.7, which can be activated or deactivated using the binary parameter d_{fix} [-].

$$d_{\text{ref}}^{\text{c}, \text{n}, \text{h}, \text{td}} = \text{End}_{\text{uses}}^{\text{c}, \text{h}, \text{td}} \quad \forall c, n, h, \text{td} \quad (3.6)$$

$$d_{\text{fix}} \cdot d^{\text{c}, \text{n}, \text{h}, \text{td}} = d_{\text{fix}} \cdot d_{\text{ref}}^{\text{c}, \text{n}, \text{h}, \text{td}} \quad \forall c, n, h, \text{td} \quad (3.7)$$

3.6.3. Perfectly inelastic demand up to VOLL

Perfectly inelastic demand up to the VOLL is the standard modeling practice and reflects the price caps used in many electricity markets [11]. In coordinated US electricity markets, for example, demand satisfaction is ensured by introducing a VOLL bid, which reflects the high societal value placed on avoiding unserved energy. This market-activating bid incentivizes supply at high prices rather than enforcing participation through constraints, thereby preserving the key economic properties of the market clearing formulation [2].

The demand curve is perfectly inelastic up to the price cap $p = \text{VOLL}$ [$\text{M}\in\text{GWh}^{-1}$], above which it becomes perfectly elastic. Demand valued at VOLL enters the objective function as consumer term $\text{VOLL} \cdot d$, which preserves the linearity of the optimization [11].

If the price exceeds VOLL, load is shed. The dependent variable d_{diff} tracks the difference between actual and reference consumer demand, as defined in Equation 3.8.

$$d_{\text{diff}}^{\text{c}, \text{n}, \text{h}, \text{td}} = d^{\text{c}, \text{n}, \text{h}, \text{td}} - d_{\text{ref}}^{\text{c}, \text{n}, \text{h}, \text{td}} \quad \forall c, n, h, \text{td} \quad (3.8)$$

With perfectly inelastic demand up to VOLL, this difference can only be zero or negative, indicating shedding, whereas under the following elastic demand curves it may also become positive, indicating overproduction.

3.6.4. Linear demand

A linear demand curve $p = a - b \cdot d$ with parameters a [$M \in GWh^{-1}$] and b [$M \in GWh^{-2}$] is the simplest way to represent demand elasticity. The corresponding consumer term in the objective function $a \cdot d - \frac{b}{2}d^2$ is quadratic [11]. The price elasticity of demand ϵ [-], defined in Equation 3.9, measures the sensitivity of demand to price [17]. A drawback of the linear demand curve is that the elasticity varies along the curve, becoming more elastic at higher prices [11]. Moreover, since a linear function only has two degrees of freedom, reference demand, reference price, elasticity, and VOLL cannot all be specified independently.

$$\epsilon = -\frac{\% \text{ change in demand}}{\% \text{ change in price}} = -\frac{\partial d / p}{\partial p / d} \quad (3.9)$$

3.6.5. Log-log demand

The demand function $d = \tilde{A}p^{-c}$ has constant elasticity c , as derived in Equation 3.10. The corresponding inverse demand function $p = Ad^\beta$ has the same constant elasticity $c = -\beta^{-1}$, with curve parameter $A = \tilde{A}^{1/c}$. Both demand functions represent the inverse log-log demand curve $\ln(p) = a - b \ln(d)$.

$$\epsilon = -\frac{\partial d / p}{\partial p / d} = -(-\tilde{A}cp^{-c-1}) \frac{p}{\tilde{A}p^{-c}} = c \quad (3.10)$$

An empirical analysis by Arnold et al. [18] finds that consumer flexibility in the German power market can be modeled using a log-log demand curve with an elasticity of 5%.

3.6.6. Piecewise linear demand

Since nonlinearities beyond quadratic terms make solving inefficient, Brown et al. [11] approximate the log-log demand curve using PWL segments. They represent all consumers using a single aggregate demand curve. Similarly, the multi-product SC EnergyScope model aggregates all consumers at the single national node into a national demand curve with uniform elasticity. However, because EnergyScope includes multi-sector coupling, a separate aggregate demand curve is specified for each end-use type.

3. Modeling

Brown et al. [11] use the same demand curve for each hour to isolate supply effects from demand. In contrast, because end-uses in EnergyScope vary over time, the multi-product SC EnergyScope model recalibrates the demand curve at each time node based on the corresponding time-varying reference demand. Together with the reference price p_{ref} [M€ GWh^{-1}], which corresponds to consumers' bid values, this allows calculating the log-log demand curve parameter according to Equation 3.11.

$$A^{c,n,h,td} = \frac{p_{\text{ref}}^{c,n,h,td}}{(d_{\text{ref}}^{c,n,h,td})^{\beta^{c,n,h,td}}} \quad \forall c, n, h, td \quad (3.11)$$

The reference demands of the consumers are equal to the end-uses, as expressed in Equation 3.6. For electricity and high-temperature heat, end-uses are fixed. However, for low-temperature heat, which is endogenously split between decentralized and district heating supply, the share supplied by district heating is a decision variable. To preserve linearity of the optimization problem, the nonlinear Equation 3.11 must be evaluated using parameters only. Consequently, end-use demand must be fully parameterized, which requires fixing the share of district heating in the multi-product SC EnergyScope model. This share is set to 37 %, corresponding to the standard outcome of the core EnergyScope model.

We approximate the inverse log-log demand curve using K PWL segments. Following Brown et al. [11], a demand multiplier d_{mult} is defined for each breakpoint $b \in \{0, \dots, K\}$ according to Equation 3.12, such that the first non-zero and final demand breakpoints d_{pwl} [GW], computed using Equation 3.13, correspond to 95 % and 110 % of the reference demand, respectively. Evaluating the log-log curve at the demand breakpoints using Equation 3.14 yields the corresponding prices p_{pwl} [M€ GWh^{-1}].

$$d_{\text{mult}}^b = \begin{cases} 0, & b = 0, \\ 0.95 + (1.1 - 0.95) \frac{b-1}{K-1}, & \text{otherwise.} \end{cases} \quad \forall b \quad (3.12)$$

$$d_{\text{pwl}}^{b,c,n,h,td} = d_{\text{mult}}^b \cdot d_{\text{ref}}^{c,n,h,td} \quad \forall b, c, n, h, td \quad (3.13)$$

$$p_{\text{pwl}}^{b,c,n,h,td} = \begin{cases} \text{VOLL,} & b = 0, \\ 0, & b = K, \\ A^{c,n,h,td} \left(d_{\text{pwl}}^{b,c,n,h,td} \right)^{\beta^{c,n,h,td}}, & \text{otherwise.} \end{cases} \quad \forall b, c, n, h, td \quad (3.14)$$

3. Modeling

For each segment $k \in \{1, \dots, K\}$, the width D [GW], slope b [M€ GWh^{-2}], and intercept a [M€ GWh^{-1}] are defined by Equations 3.15, 3.16, and 3.17.

$$D^{k,c,n,h,td} = d_{\text{pw}}^{k,c,n,h,td} - d_{\text{pw}}^{k-1,c,n,h,td} \quad \forall k, c, n, h, td \quad (3.15)$$

$$b^{k,c,n,h,td} = \frac{p_{\text{pwl}}^{k-1,c,n,h,td} - p_{\text{pwl}}^{k,c,n,h,td}}{D^{k,c,n,h,td}} \quad \forall k, c, n, h, td \quad (3.16)$$

$$a^{k,c,n,h,td} = p_{\text{pwl}}^{k-1,c,n,h,td} \quad \forall k, c, n, h, td \quad (3.17)$$

The resulting PWL demand curve approximates a log-log demand curve, as shown in Figure 3.5. Moreover, at zero demand, the price equals VOLL, while at zero price the maximum demand reaches 110 % of the reference demand. The assumed VOLL is 11030 € MWh^{-1} , corresponding to the median estimate for Germany reported by Kachirayil et al. [19]. The zoomed panel highlights the PWL approximation around the reference point, where the empirical demand elasticity of 5 % determines consumer behavior.

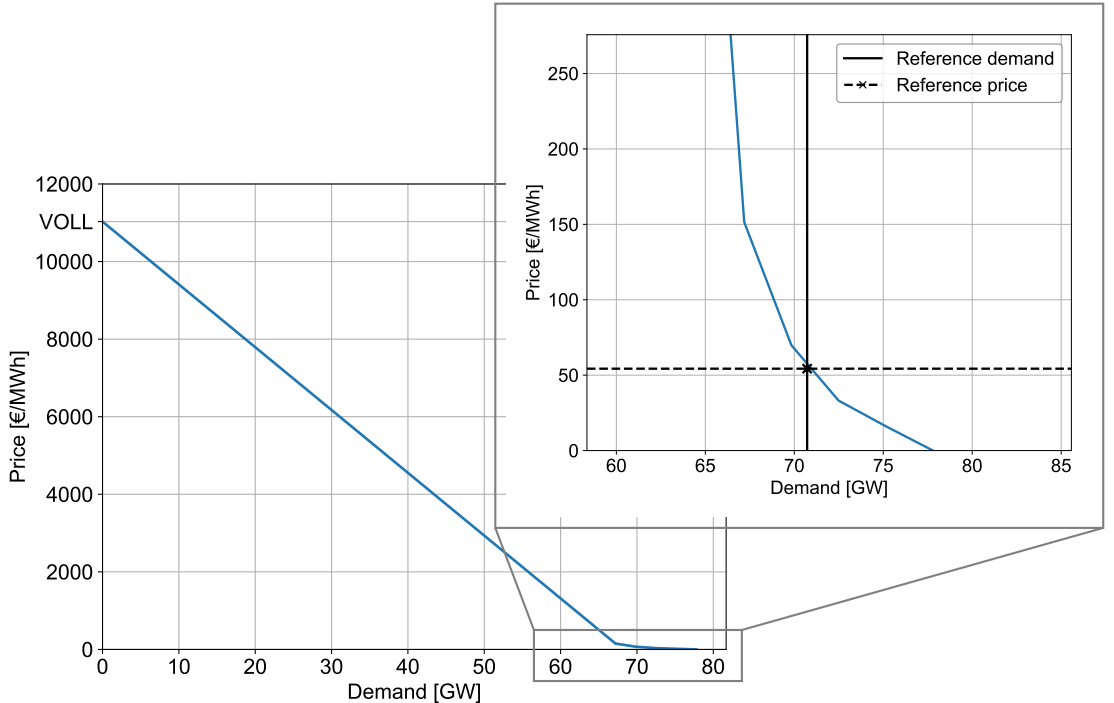


Figure 3.5.: Electricity demand curve zoomed in around the reference point.

3. Modeling

Figure 3.6 compares the price elasticity along our five-segment PWL demand curve to the three-segment demand curve of Brown et al. [11]. Over the range from 95 % to 110 % of the reference demand, elasticity oscillates around 5 % before declining to zero at the maximum demand. In the opposite direction, as prices increase toward the VOLL at zero demand, elasticity increases. As discussed in Section 3.6.4, this is a drawback of linear demand curves, however, for PWL demand curves it can be limited to less frequent demand levels. The PWL demand curve might be further improved with fully elastic demand below the 95 % segment at the VOLL, rather than a linear increase toward the VOLL.

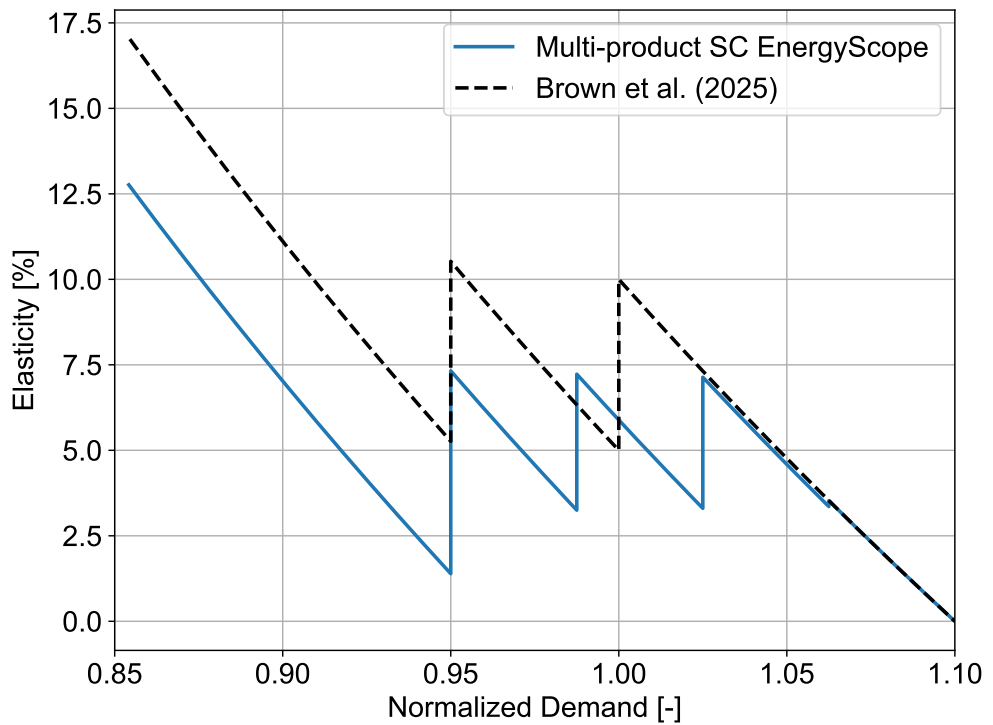


Figure 3.6.: Elasticity along PWL demand curve [11].

Constraints 3.18 and 3.19 govern consumer behavior along the elastic demand curve. Constraint 3.18 bounds the demand in each segment d_{seg} [GW]. Constraint 3.19 then aggregates the demand across all segments to the consumer demand.

$$d_{\text{seg}}^{k,c,n,h,td} \leq D^{k,c,n,h,td} \quad \forall k, c, n, h, td \quad (3.18)$$

$$\sum_k d_{\text{seg}}^{k,c,n,h,td} = d^{c,n,h,td} \quad \forall c, n, h, td \quad (3.19)$$

3.7. Objective function

Figure 3.7 illustrates the market situation in the multi-product SC EnergyScope model. Based on this visualization, the following section compares the objective of minimizing total system cost in the core EnergyScope model with maximizing social welfare in the multi-product SC EnergyScope model.

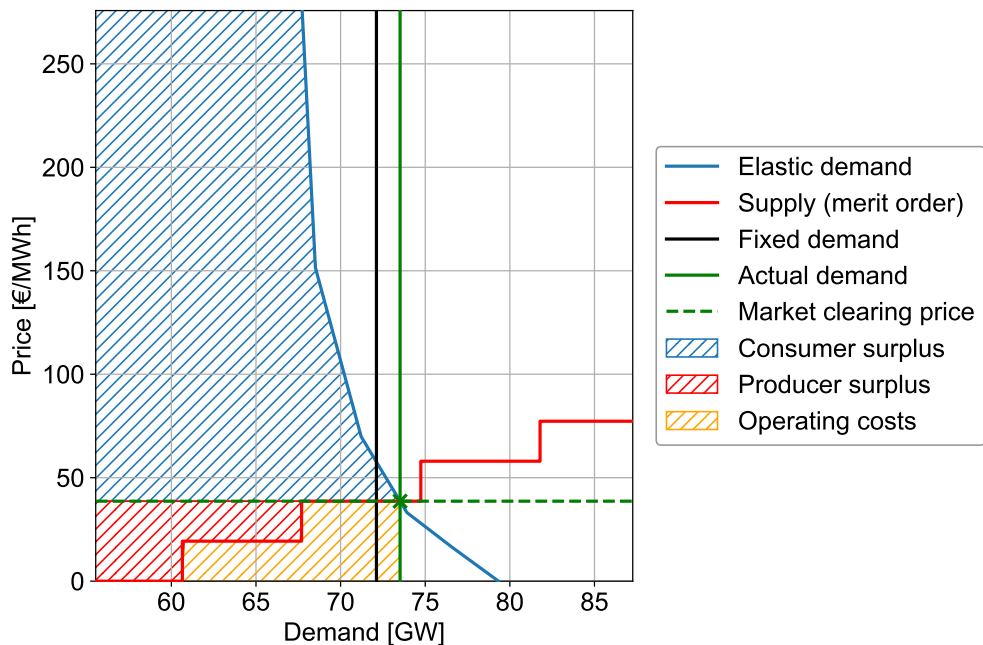


Figure 3.7.: Market situation in the multi-product SC EnergyScope model.

3.7.1. Total cost

The core EnergyScope model minimizes the total system cost TotalCost [M€ a^{-1}], defined in Equation 3.20 as the sum of resource operating costs and technology investment as well as O&M costs. Investment costs are annualized for each technology using the factor τ [a^{-1}]. The resulting core EnergyScope optimization problem is a LP.

$$\min \text{TotalCost} = \sum_i C_{\text{op}}^i + \sum_j (\tau^j C_{\text{inv}}^j + C_{\text{maint}}^j) \quad (3.20)$$

3.7.2. Social welfare

The total surplus is the sum of consumer and producer surpluses and corresponds to the area between the demand and supply curves, as shown in Figure 3.7. In the multi-product SC EnergyScope model, Social welfare SocialWelfare [$M\text{€ a}^{-1}$] is equal to the total surplus minus technology investment and O&M costs, as expressed in Equation 3.21. For an elastic PWL demand curve, the consumer surplus term becomes quadratic, as illustrated in Figure 3.8, which transforms the optimization problem from a LP into a quadratic program (QP). Since processors and transporters submit zero bids, as discussed in Section 3.5, on the producer side only the suppliers bids remain from the objective function of the multi-product SC framework shown in Figure 2.3.

$$\max \text{SocialWelfare} = \sum_{n,h,td} w^{h,td} t_{op}^{h,td} \left[\sum_{c,k} \left(a^{k,c,n,h,td} d_{seg}^{k,c,n,h,td} - \frac{1}{2} b^{k,c,n,h,td} (d_{seg}^{k,c,n,h,td})^2 \right) - \sum_s (c_{op}^s g^{s,n,h,td}) \right] - \sum_j (\tau^j C_{inv}^j + C_{maint}^j) \quad (3.21)$$

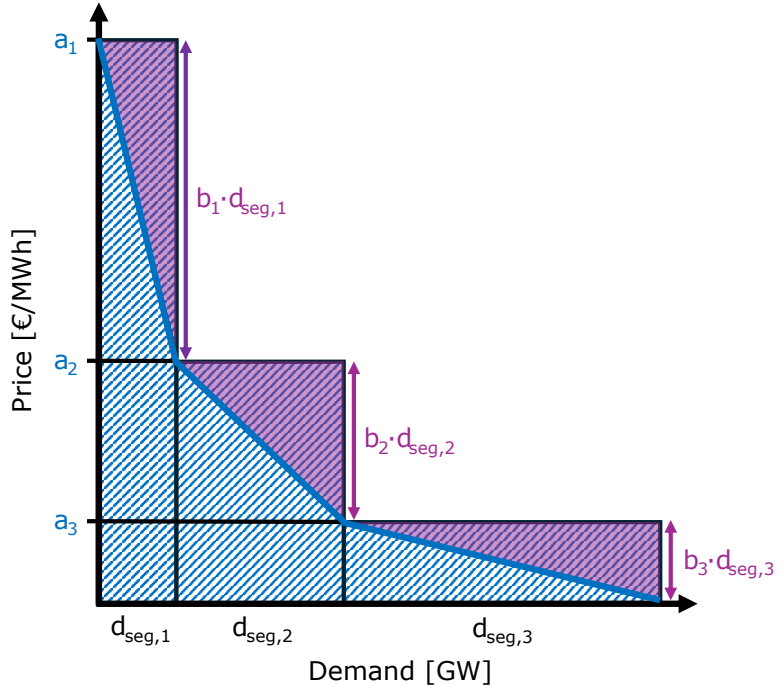


Figure 3.8.: Illustration of quadratic PWL consumer term in the objective function.

4. Case Study

This chapter presents the results of the multi-product SC EnergyScope model applied to a single-node representation of Germany's national energy system in 2050, focusing on the coupled electricity and heating sectors.

4.1. Data

We obtain the input data from the Python for Power System Analysis Europe (PyPSA-Eur) workflow adapted to the EnergyScope framework [20, 21]. A detailed explanation of the data extraction, preprocessing, and integration steps is provided by the semester project "Bridging the Modeling Gap: Automating Data Flow from PyPSA to EnergyScope" developed by Till Cassens. For illustration, Figures 4.1 and 4.2 present the capacity factor heat maps for photovoltaic (PV) and onshore wind generation, respectively.

4.2. Price scenarios

Initially, we run the model assuming a demand elasticity of 5%, consistent with empirical estimates for the German electricity market reported by Arnold et al. [18]. In this base case, we impose an emission cap equal to 25% of the unconstrained emission level. This choice is intended to align with Germany's 2045 net-zero target [22], while acknowledging that the model does not incorporate negative emission technologies. Using the dual variables π [€ MWh^{-1}] of the balance constraint in Equation 3.2, we then compute yearly average end-use prices $\bar{\pi}^{eut}$ [€ MWh^{-1}], according to Equation 4.1.

$$\bar{\pi}^{eut} = \frac{\sum_{h,td} \pi^{eut,h,td} w^{h,td} t_{op}^{h,td}}{\sum_{h,td} w^{h,td} t_{op}^{h,td}} \quad \forall eut \quad (4.1)$$

4. Case Study

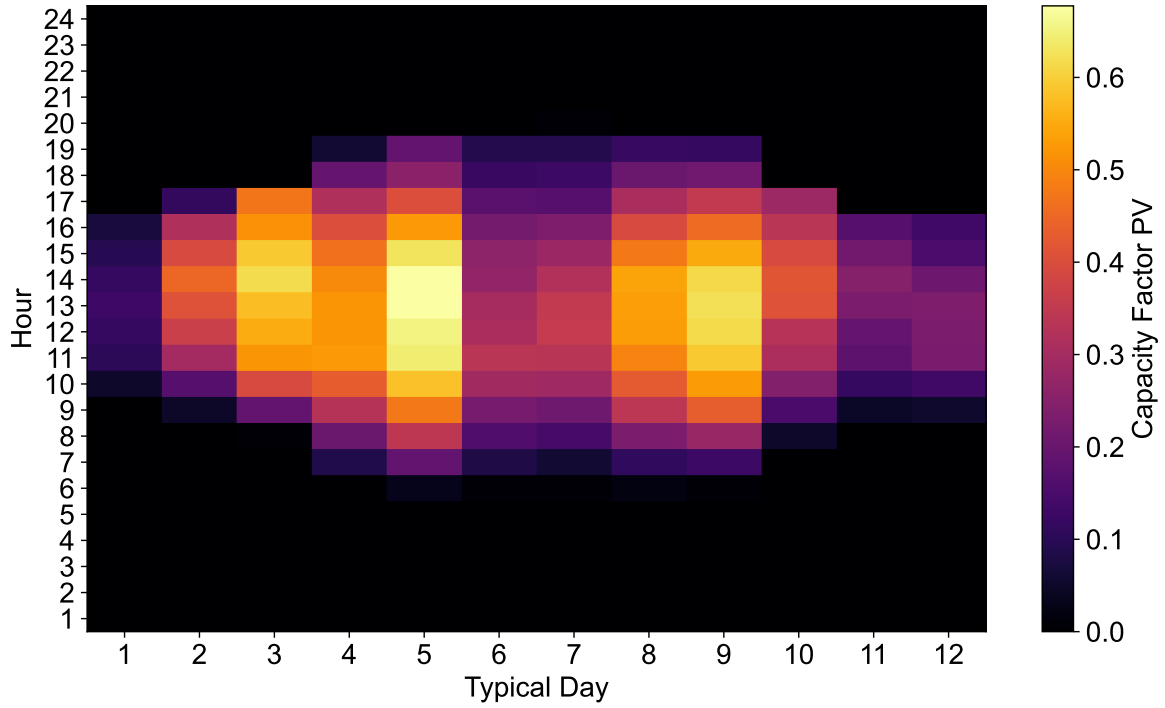


Figure 4.1.: Capacity factor heat map for PV.

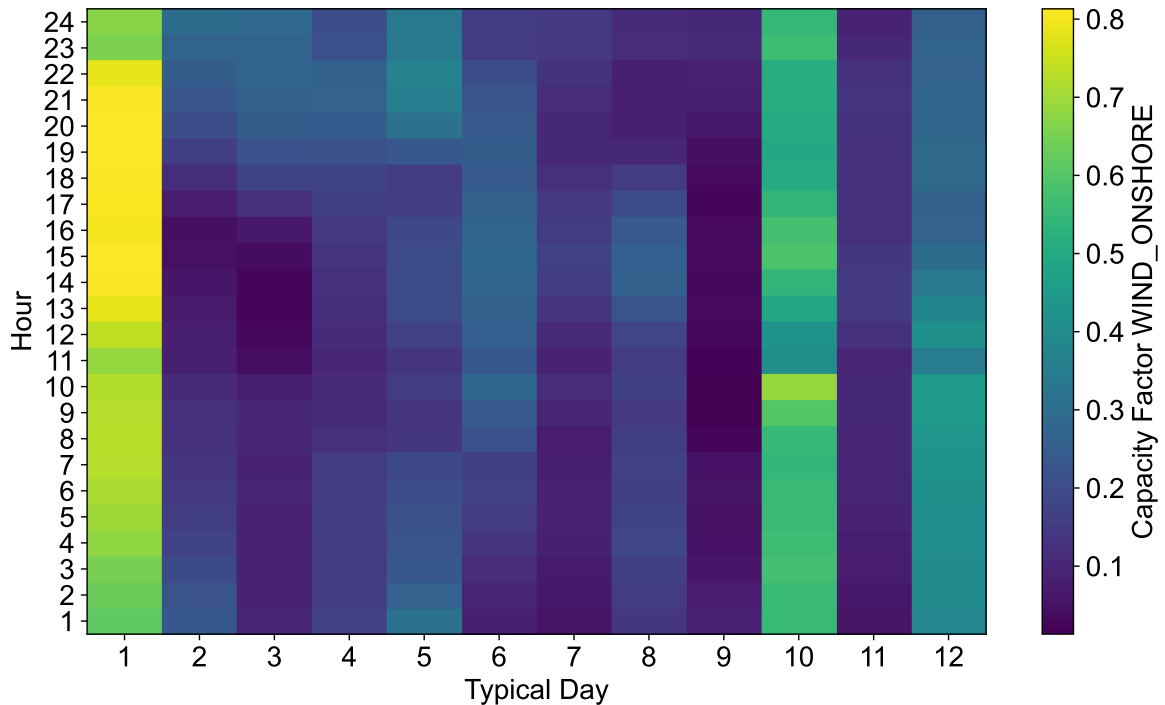


Figure 4.2.: Capacity factor heat map for onshore wind.

4. Case Study

The resulting prices constitute the normal-price level for all end-use types. Using this as a reference, we generate two additional scenarios in which the normal prices are halved to form a low-price level and doubled to form a high-price level. Table 4.1 reports the yearly average end-use prices for all three scenarios. These values are subsequently used as consumer bids and serve as the reference prices for the elastic demand curves.

End-use type	Price scenario [€/MWh]		
	Low	Normal	High
Electricity	27.15	54.30	108.60
Heat _{highT}	15.83	31.67	63.33
Heat _{lowT,DHN}	7.90	15.80	31.61
Heat _{lowT,DECEN}	14.27	28.54	57.08

Table 4.1.: Yearly average end-use prices for low-, normal-, and high-price scenarios.

4.3. Demand elasticity

We perform a sensitivity analysis on the price elasticity of demand, introducing flexible consumer behavior. Following Brown et al. [11], we consider elasticities of -2.5% , -5% , and -10% , along with a fully inelastic reference case, as shown in Figure 4.3.

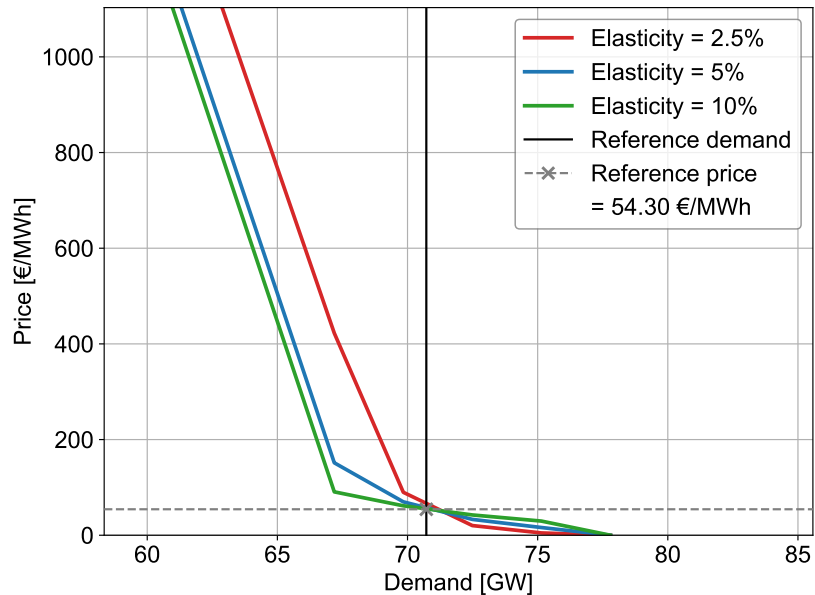


Figure 4.3.: Demand curves with different elasticities for the normal-price scenario.

4. Case Study

Figure 4.3 shows that the reference point does not necessarily lie on the PWL demand curve. Since no breakpoint coincides with the reference demand, the exact reference point is not evaluated using the log-log relationship in Equation 3.14. As shown in Figure 3.6, this avoids the large elasticity jump at the reference point observed by Brown et al. [11].

Under the simplifying assumption that, in a highly electrified 2050 German energy system, the heating sector is strongly coupled to the electricity sector, we apply the same elasticity used for electricity to all heating end-use types. For each elasticity, we compute an ε -constrained Pareto front with respect to global warming potential (GWP), capturing the trade-off between social welfare and progressively tighter emission constraints.

As shown in Section 3.7, introducing a PWL elastic demand curve makes the otherwise linear multi-product SC framework quadratic, thus, we assess whether this affects solve times. The multi-product SC EnergyScope model is formulated as a continuous QP in AMPL [23] and solved using Gurobi [24]. Figure 4.4 reports solve times along the Pareto front under the normal-price scenario. For fixed demand, the additional constraint in Equation 3.7 is introduced, while the objective function remains quadratic. To assess whether replacing a linear with a quadratic objective affects computation time, the figure also includes solve times from a comparable core version of EnergyScope evaluated under the same emission constraints. Across all runs, solve times range between 15s and 28s, with no systematic differences between the linear and quadratic formulations or across elasticity settings.

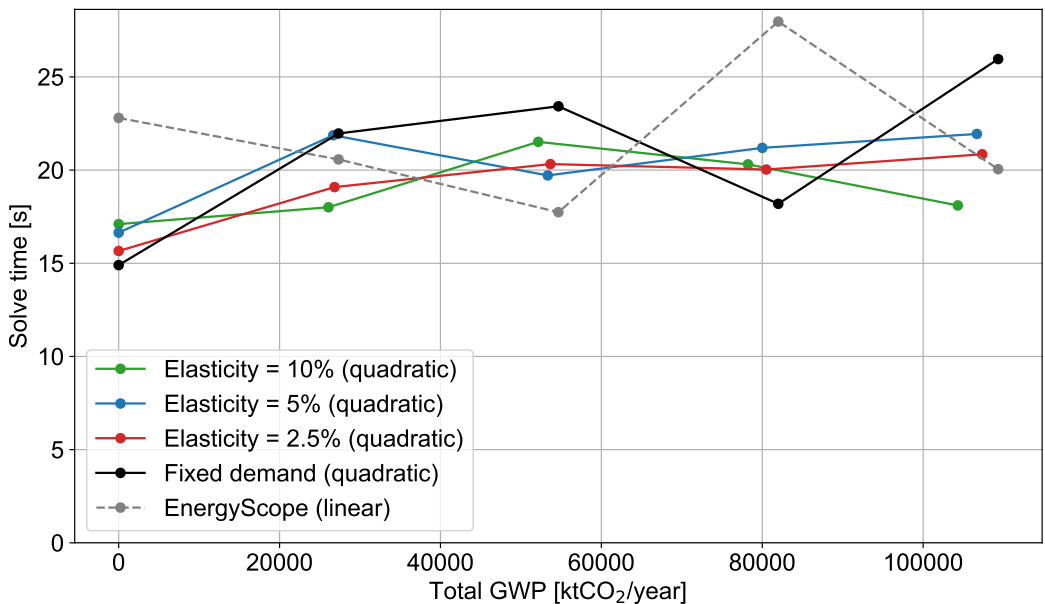


Figure 4.4.: Solve time versus GWP for the normal-price scenario.

4. Case Study

Figure 4.5 shows the social welfare Pareto fronts for the normal-price scenario. Each elasticity curve is normalized with respect to its own unconstrained emission case. As the emission constraint becomes tighter, higher elasticities lead to smaller welfare reductions, suggesting that demand flexibility softens the trade-off between sustainability and welfare. However, even after normalization, the trade-off remains small both within each elasticity curve and across elasticity cases. This is consistent with the strong alignment of economic and environmental objectives in a system where renewable technologies tend to be the most favorable options both economically and in terms of emissions.

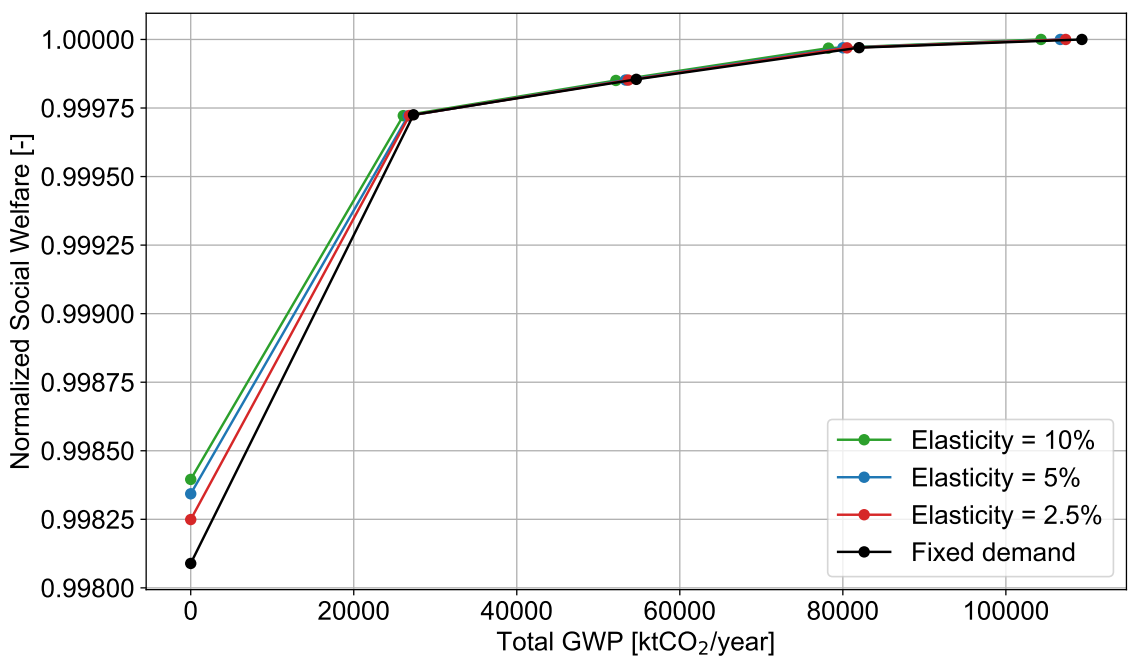


Figure 4.5.: Normalized social welfare versus GWP for normal-price scenario.

Although the model has the objective to maximize social welfare, examining the resulting total system costs provides valuable insight into the investment choices implied by each scenario. Figure 4.6 shows total system cost as a function of GWP across different demand elasticities. For the low-price scenario, a higher elasticity leads to lower total system costs. When the reference price falls below the actual price, stakeholders prefer to supply less than the reference demand, as illustrated in the demand curve in Figure 4.7. Greater elasticity allows consumers to shed more load at a lower price penalty, reducing the need for capacity expansion. In contrast, when the reference price exceeds the actual price, stakeholders prefer to supply more than the reference demand, as shown in Figure 4.8.

4. Case Study

Under the high-price scenario, increased elasticity enables consumers to express a higher WTP, encouraging stakeholders to provide more energy. Consequently, more capacity is built, and total system costs rise with increasing elasticity. An exception occurs under zero emissions. Even in the high-price scenario, meeting demand becomes too costly, so higher elasticity results in reduced demand and therefore lower capacity expansion, ultimately decreasing total costs. In summary, the model captures demand-side flexibility through price-elastic consumer behavior. In competitive market conditions, suppliers and processors can respond strategically to this flexibility, adjusting both investment and operational decisions to maximize overall social welfare.

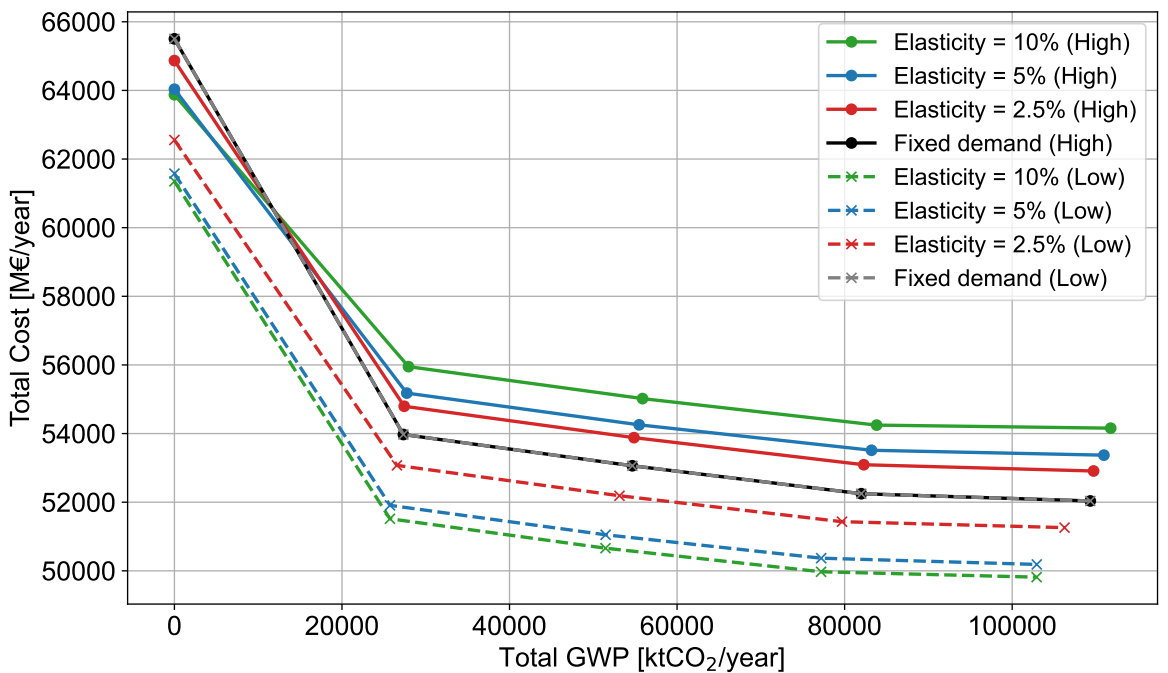


Figure 4.6.: Total system cost versus GWP for high- and low-price scenarios.

Special attention should be drawn to the fixed demand cases in Figure 4.6. Both the low-price and the high-price scenarios lead to exactly the same total system cost, because the system must satisfy a predetermined quantity of energy regardless of price levels. Under such conditions, the consumer term of the objective function in Equation 3.21 becomes constant. Since demand no longer reacts to price signals, consumer bids no longer influence the optimization decisions and only rescale the objective. Removing the consumer term reduces the objective function to the cost minimization form shown in Equation 4.2 without affecting the resulting system outcome.

4. Case Study

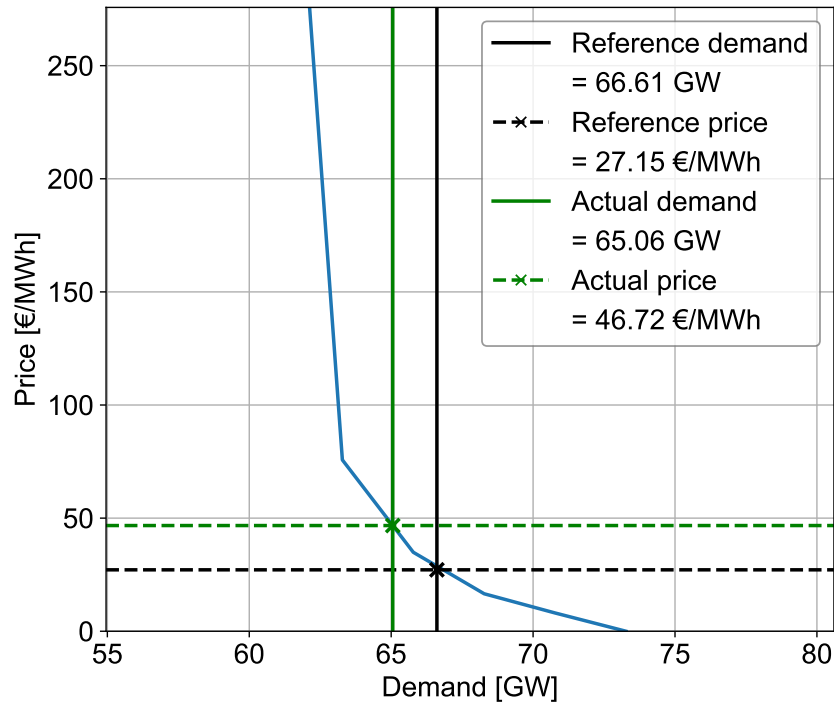


Figure 4.7.: Electricity demand curve for the low-price scenario in hour 19 of TD 8.

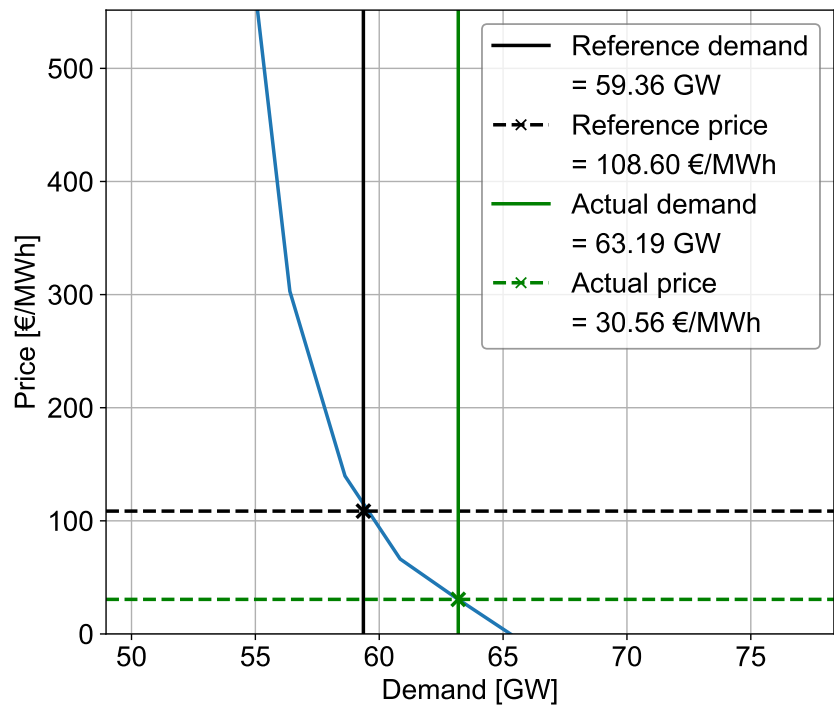


Figure 4.8.: Electricity demand curve for the high-price scenario in hour 1 of TD 6.

4. Case Study

$$\begin{aligned} \max \text{SocialWelfare} &= - \sum_{s,n,h,td} (c_{\text{op}}^s g^{s,n,h,td} w^{h,td} t_{\text{op}}^{h,td}) - \sum_j (\tau^j C_{\text{inv}}^j + C_{\text{maint}}^j) \\ \Leftrightarrow \min \text{TotalCost} &= \sum_i C_{\text{op}}^i + \sum_j (\tau^j C_{\text{inv}}^j + C_{\text{maint}}^j) \end{aligned} \quad (4.2)$$

The only remaining driver of the optimization is the structure of supply side costs. Consequently, when demand is perfectly inelastic, maximizing social welfare and minimizing total system cost produce the same solution. The linear equilibrium formulation therefore collapses to the standard EnergyScope framework. This relates directly to the work of Tominac et al. [2], introduced in Section 2.1, who show that forcing stakeholder participation destroys the economic properties that define a coordinated market equilibrium.

Importantly, this result is unaffected by the level of detail used to represent supply side stakeholders. As long as demand is fixed and fully inelastic, even disaggregating supply technologies into many individual stakeholders does not introduce meaningful price quantity interactions within a linear market clearing formulation. For instance, modeling each coal power plant in Germany as a separate bidder with its own MC would still lead the welfare maximizing and cost minimizing formulations with the same level of granularity to produce the same system configuration. Under fixed demand, the equilibrium remains entirely determined by supply side costs and no new strategic interactions emerge.

Differences between social welfare maximization and total cost minimization only arise once consumer bids are allowed to vary. As discussed in Section 3.6, the most straightforward way to introduce such variation while preserving linearity is to represent demand as a vertical curve capped at VOLL, allowing demand to be shed when prices exceed this threshold. In practice, however, electricity systems are engineered to avoid load shedding. For example, the German Bundesnetzagentur reports that in 2024 the average non-availability of electricity was only 11.7 minutes [25]. Moreover, models based on TDs, such as EnergyScope, might miss the extreme conditions under which shedding might occur. As a result, market prices almost never reach VOLL, no demand is shed, and the optimized consumption remains identical to the fixed demand. Under these circumstances, introducing an inelastic demand curve with VOLL yields again the same solution as the fixed demand EnergyScope formulation, since a zero shedding outcome is indistinguishable from fixed demand.

4.4. Electricity Prices

In the following section, we analyze how the endogenous electricity prices of the multi-product SC EnergyScope model evolve across different emission levels and over time in the normal-price scenario, with particular attention to zero-price and peak-price hours.

4.4.1. Dependence on Emission Cap

Figure 4.9 shows how the emission cap influences electricity prices. As expected, tighter emission constraints lead to higher yearly average prices. Because the model excludes negative emission technologies, prices under zero emission constraint increase sharply. For any given emission cap, higher demand elasticity lowers electricity prices, as consumers adjust demand in response to price signals and thereby are able to mitigate high prices.

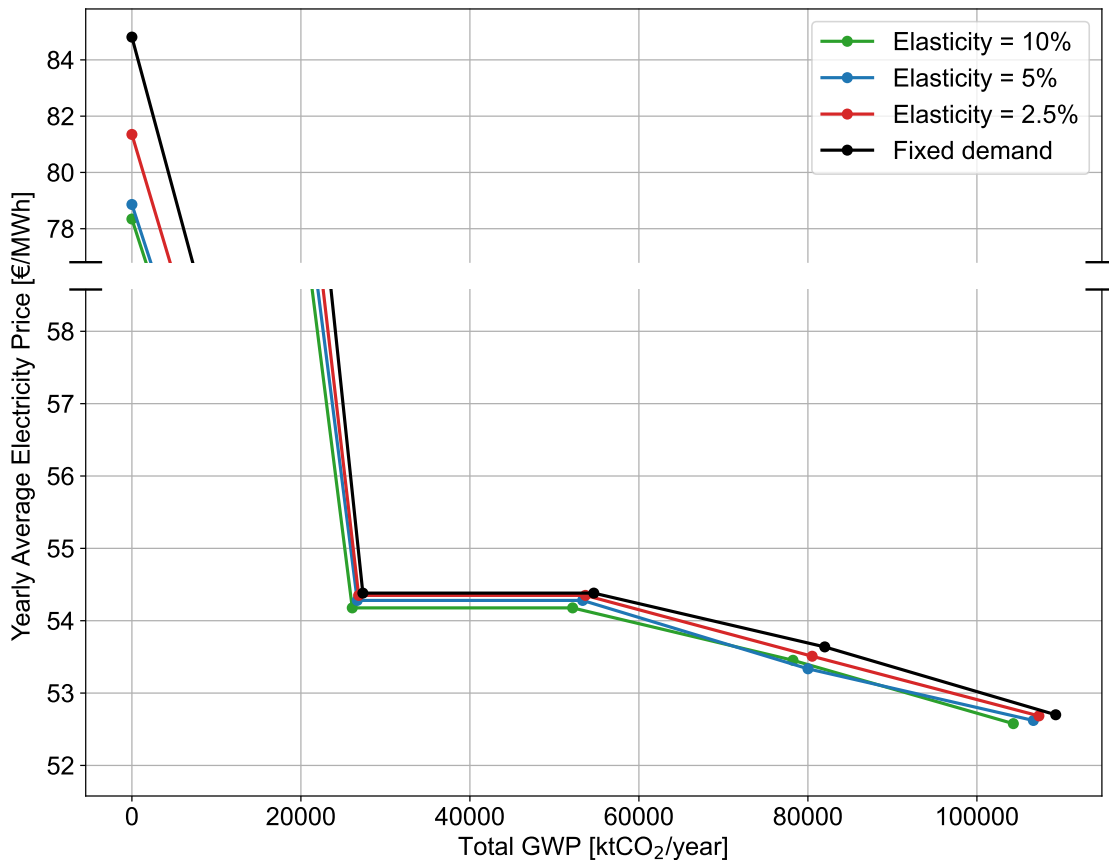


Figure 4.9.: Yearly average electricity price versus GWP for the normal-price scenario.

4.4.2. Daily profile of electricity prices

Average typical day

Figure 4.10 shows the hourly electricity price averaged over all TDs for the normal-price scenario under the zero emission constraint. All elasticity cases, including fixed demand, display the same daily pattern, with a pronounced midday dip driven by high solar generation, as indicated by the PV heatmap in Figure 4.1. Consistent with Figure 4.9, higher demand elasticity lowers electricity prices.

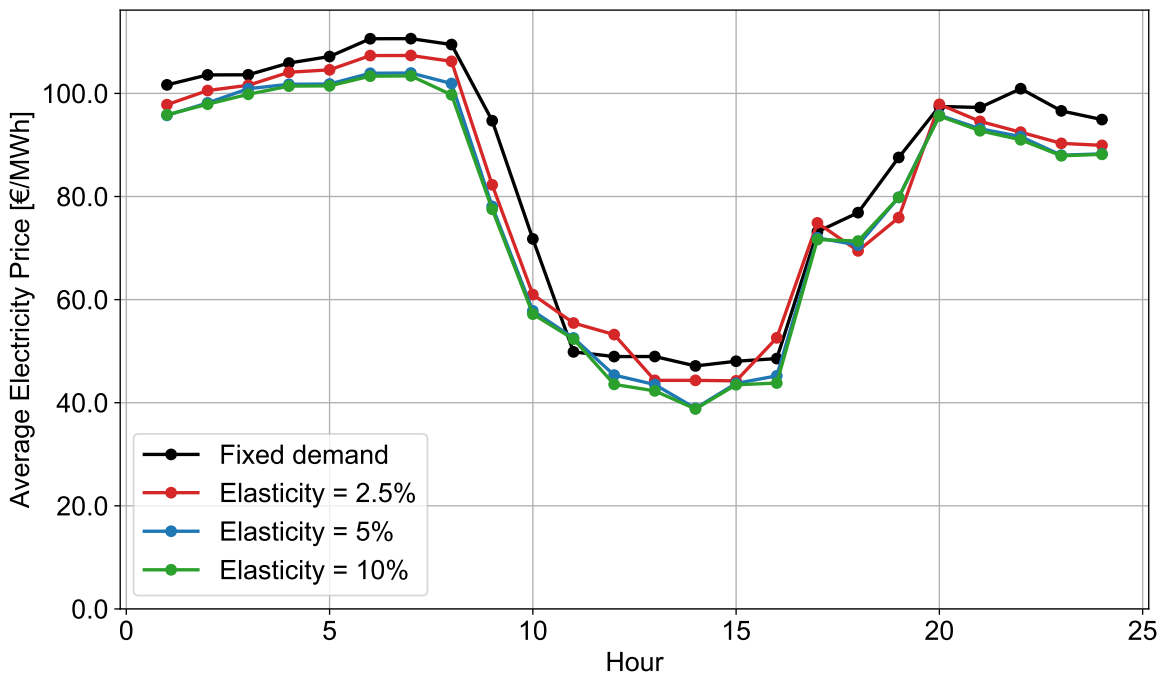


Figure 4.10.: Hourly electricity price averaged over all TDs for the normal-price zero-emission scenario.

Individual typical days

As the following figures show, hourly prices on individual TDs reflect diverse system dynamics. Interpreting the resulting price patterns requires considering the operating conditions faced by fossil and renewable suppliers, energy processors, storage units, and consumers. The capacity factor heatmaps of the dominant technologies, PV and onshore wind, in Figures 4.1 and 4.2 provide an insight into the renewable availability. A more detailed view of price formation is provided by the stakeholder flows shown in Figure 4.12 for TD 3 and in Appendix B for the other presented TDs.

4. Case Study

TD 3 represents a cold day in early spring with high heating demand and varying renewable availability throughout the day. The day begins with slight wind during the night and morning, followed by sunny but less windy conditions during daytime hours, and strong winds emerging in the evening. As a result, different technologies become marginal over the course of the day, and TD 3 exhibits three distinct electricity price levels, as shown in Figure 4.11. These price levels closely reflect the changes in renewable availability over the day, shown together with the associated shifts in marginal technologies in Figure 4.12.

The high price level during the first ten hours reflects the need for biomass and wood cogeneration. As district heating demand can be met solely by heat pumps and seasonal storage, biomass cogeneration is phased out, reducing prices, while wood cogeneration remains as the only non-zero MC technology supplying electricity.

With the onset of strong evening winds, electricity is fully supplied by zero MC technologies, leading to a further price reduction. Excess renewable generation is stored in batteries, which keeps the electricity price above zero. In the final hour of the day, increased demand enabled by flexible consumers is essential to maintain a non-zero price. By contrast, under fixed demand, zero MC renewable generation exceeds both demand and battery charging capacity, causing the electricity price to fall to zero.

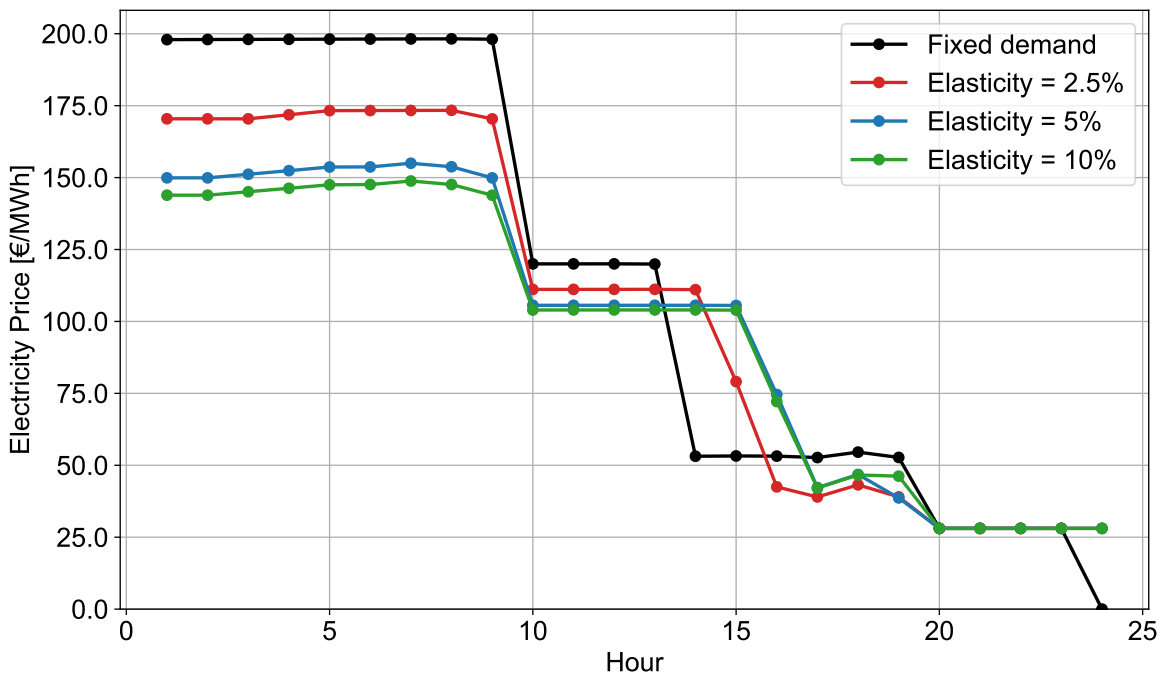


Figure 4.11.: Hourly electricity price on TD 3 for the normal-price zero-emission scenario.

4. Case Study

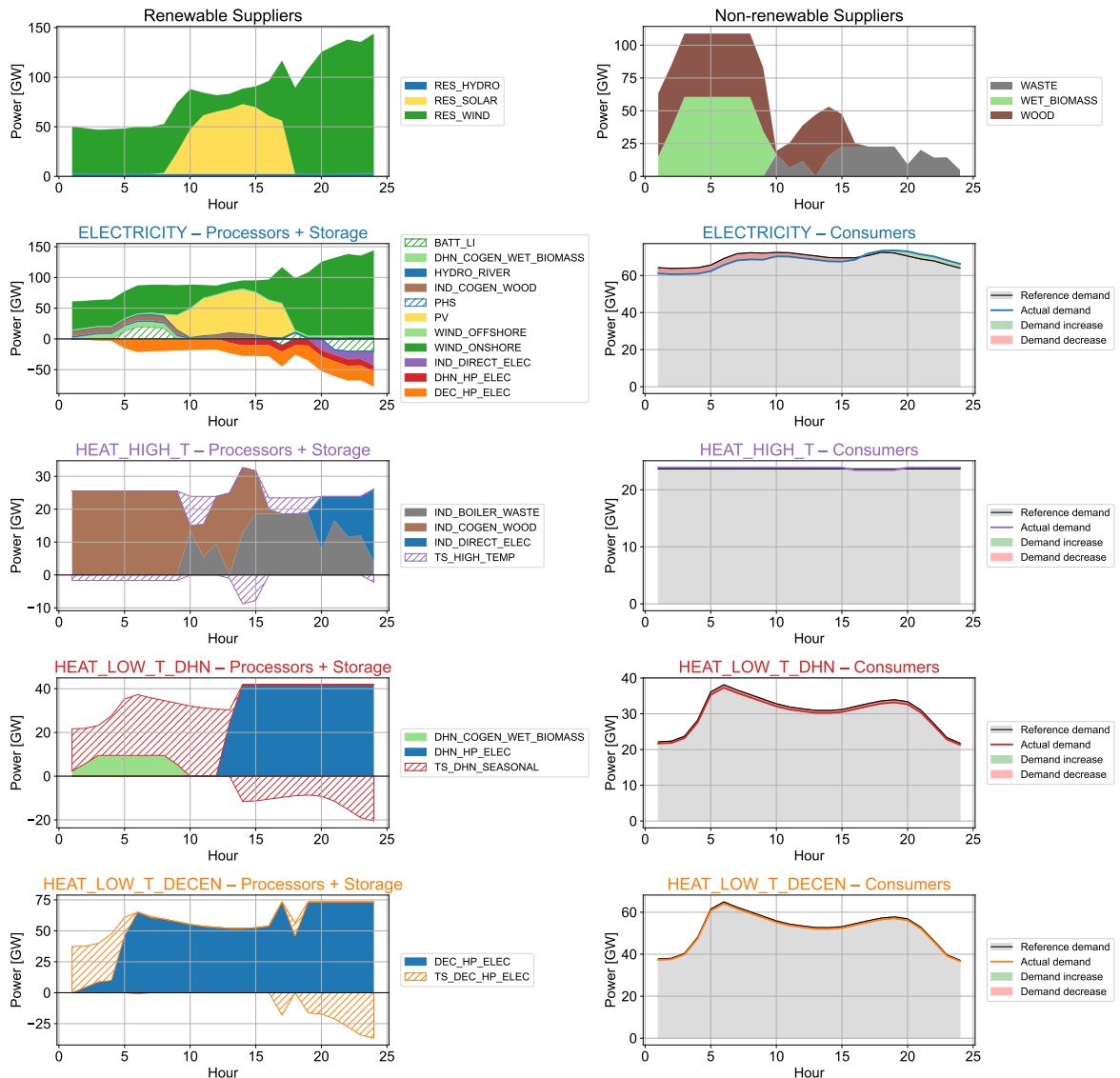


Figure 4.12.: Stakeholder flow on TD 3 for the normal-price zero-emission scenario.

4. Case Study

On TD 9, shown in Figure 4.13, storage sets the electricity price. As discussed in Section 3.5, storage technologies can set market prices by effectively bidding like generators. In place of fuel costs, their implicit MC is given by their MSV [11].

Although wood and biomass generation with non-zero MC operate continuously at full capacity, as shown in Figure B.1, and are therefore not marginal, electricity prices vary substantially over the day. This variation is driven by the charging and discharging behavior of the lithium-ion battery, shown in Figure 4.14 for an elasticity of 5 %. Hours 1 and 22–23 correspond to a charging price level of around 350 € MWh^{-1} , while hours 2–8 and 18–21 reflect a discharging price level of around 390 € MWh^{-1} . During the lower price period from hour 9 to 17, the battery charges continuously. As the battery approaches its maximum SoC toward the end of this period, the MSV is reduced. Throughout this lower price period, prices are pushed down to around 210 € MWh^{-1} .

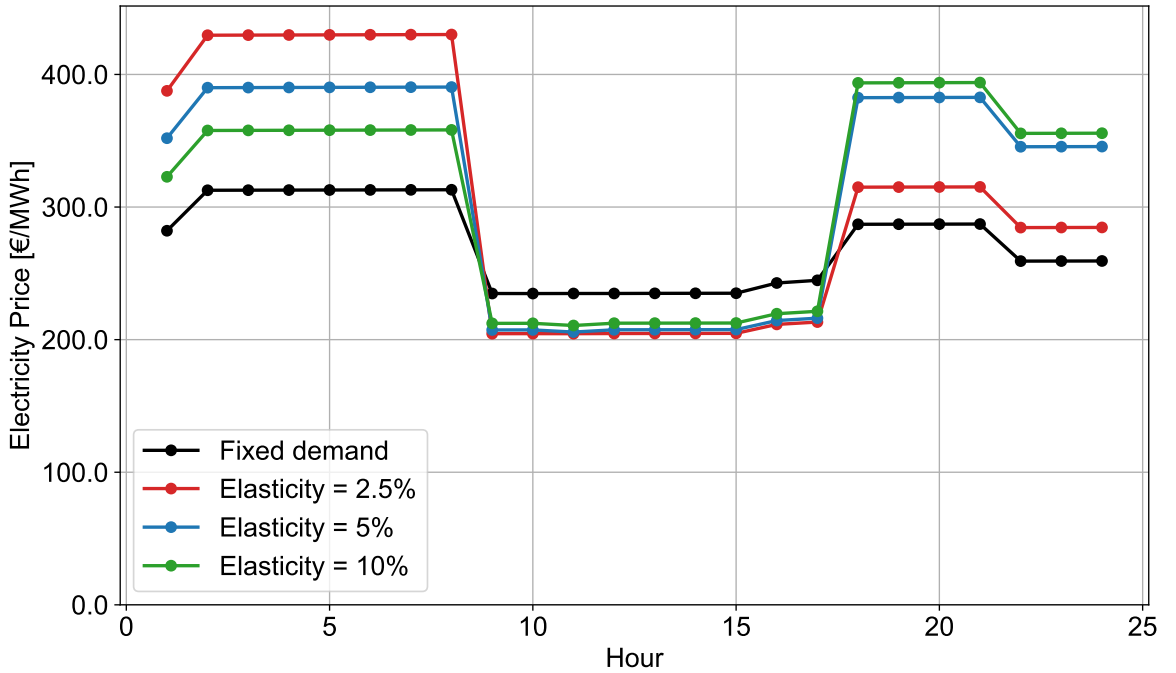


Figure 4.13.: Hourly electricity price on TD 9 for the normal-price zero-emission scenario.

On TD 9, flexible consumers amplify price volatility. Relative to the reference demand, increasing demand moves the equilibrium to the right along the demand curve, reducing prices, while decreasing demand moves it to the left, increasing prices. In contrast, on TDs 4 and 11, elastic demand can help stabilize prices by sufficiently changing demand and thereby influencing the activation of marginal plants.

4. Case Study

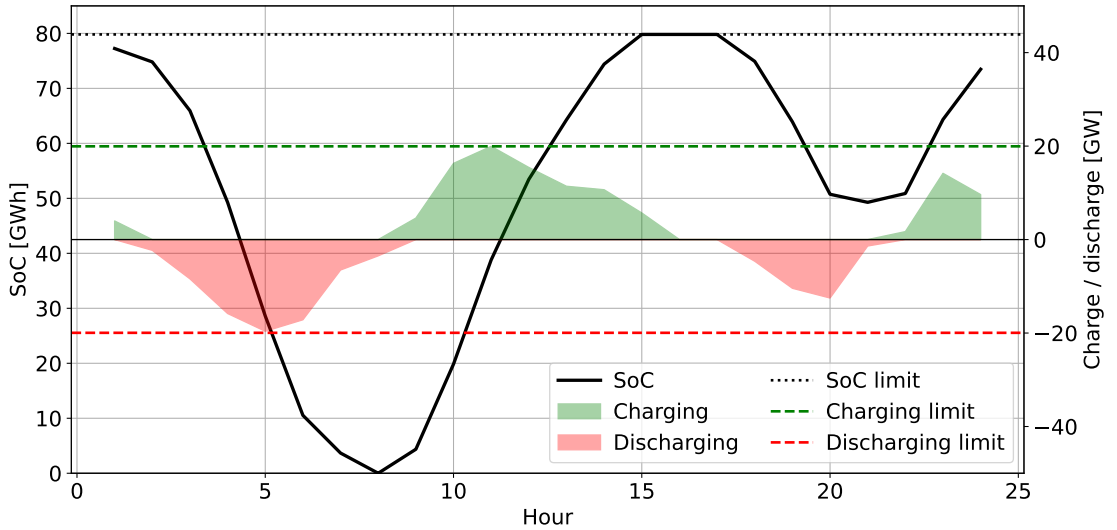


Figure 4.14.: Hourly charging, discharging, and SoC of lithium-ion battery on TD 9 for the normal-price zero-emission scenario with 5 % elasticity.

For example, on TD 4 in Figure 4.15 elastic consumers maintain stable non-zero electricity prices at times when fixed demand results in zero-price hours. A comparison of the inelastic and 5 % elastic stakeholder flows in Figures B.2 and B.3 shows that an industrial waste boiler is only activated under elastic demand. With fixed demand, the boiler remains inactive, causing electricity prices to remain zero.

Nevertheless, on several TDs such as the sunny day 5 and the very windy days 1, 10, and 12, abundant renewable generation far exceeds both demand and storage charging capacity. Throughout these days, demand elasticity is insufficient to sustain stable non-zero prices, and electricity prices remain zero.

Conversely, on TD 11 in Figure 4.16, characterized by very high winter demand and very low renewable generation, elastic demand mitigates peak-prices. To meet the fixed low temperature district heating demand, wood cogeneration must be activated, as shown in Figure B.4. Under 5 % demand elasticity, as shown in Figure B.5, consumers are able to decrease demand, thereby avoiding the activation of the higher cost marginal plant and reducing peak electricity prices

These results align with the findings of Brown et al. [11], who analyze wind and PV generation together with battery and hydrogen storage. Introducing demand elasticity in their model mitigates price bifurcation by reducing the share of zero price hours from 89 % to 31 % and the share of peak price hours above 400 € MWh^{-1} from 8.5 % to 3.9 %.

4. Case Study

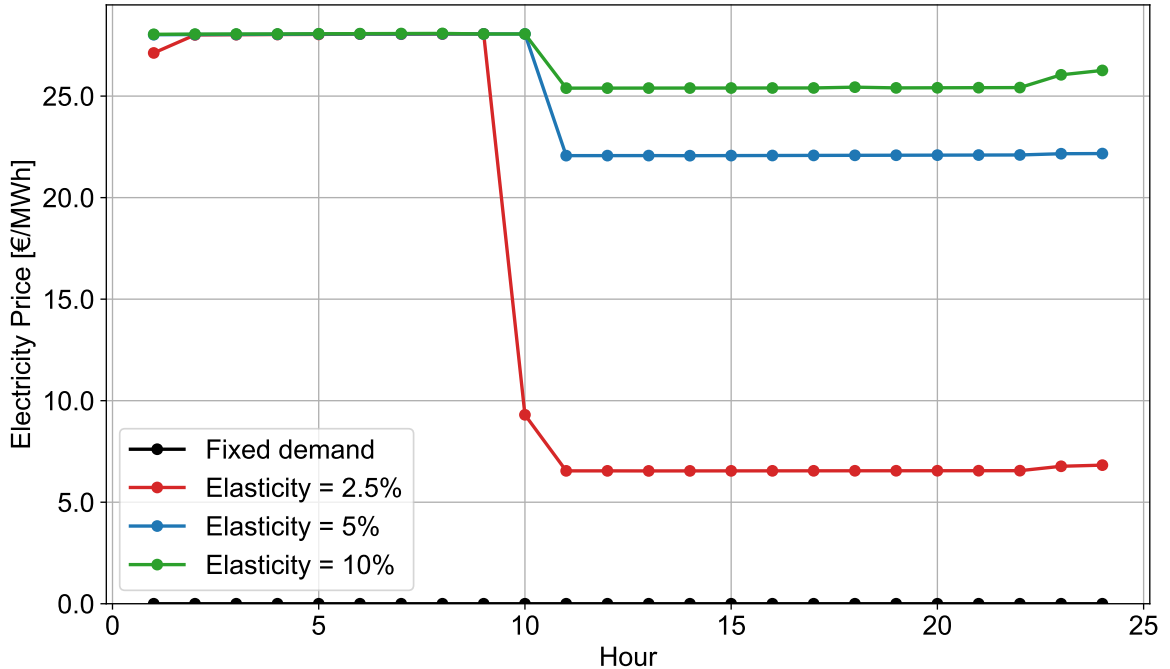


Figure 4.15.: Hourly electricity price on TD 4 for the normal-price zero-emission scenario.

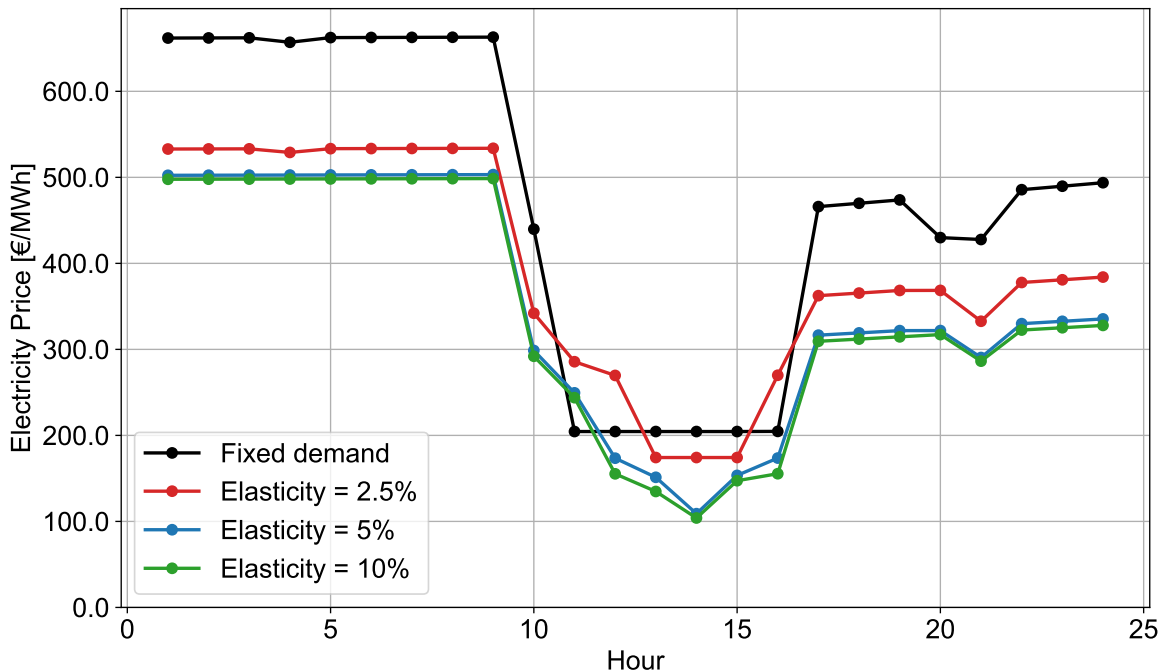


Figure 4.16.: Hourly electricity price on TD 11 for the normal-price zero-emission scenario.

4.4.3. Zero- and peak-price hours

Figure 4.17 shows the number of zero-price electricity hours per year as a function of GWP in the normal-price scenario. Allowing demand to respond to prices reduces the number of zero-price hours. For example, under zero emissions, zero-price hours decrease from 5450 (62 %) with fixed demand to 4000 (46 %) with elastic demand. With fixed demand, prices fall to zero whenever zero MC generation exceeds demand and storage charging capacity. With elastic demand, consumers can increase consumption. If this activates a technology with non-zero MC, that technology sets a positive price.

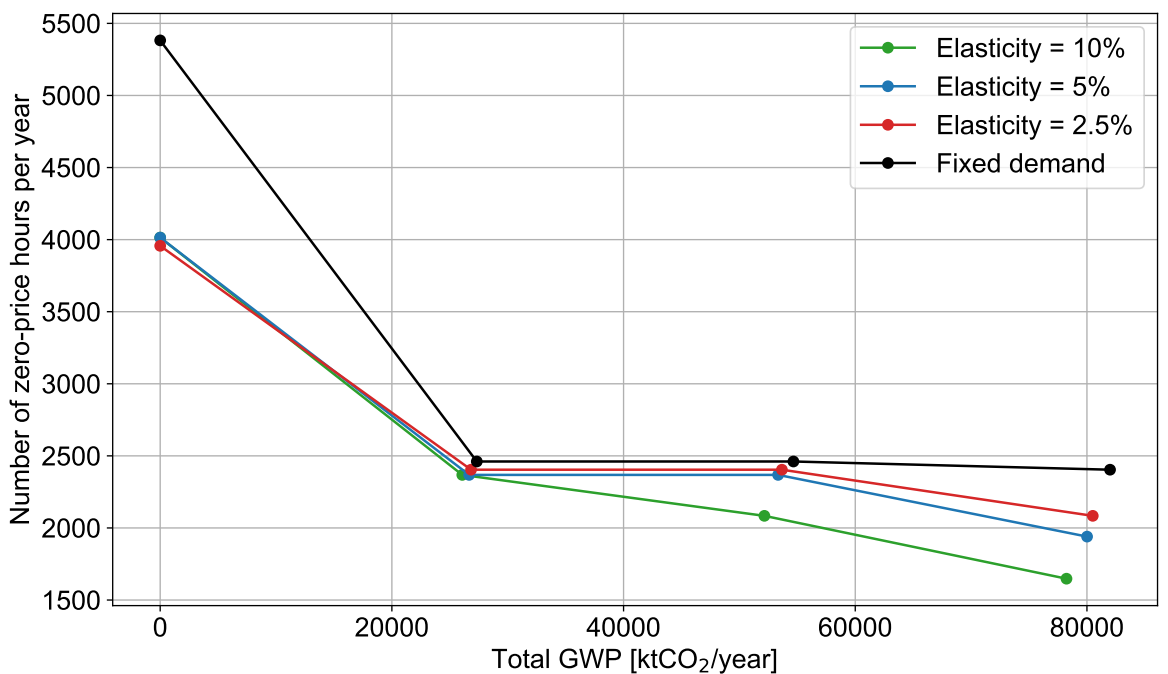


Figure 4.17.: Number of zero-price hours per year versus GWP in the normal-price scenario.

A tighter emission constraint increases the number of zero-price hours because the system relies more strongly on renewable technologies with zero MC. Figure 4.18 compares the renewable supply share under zero and unconstrained emissions for an elasticity of 5 %. As expected in a greenfield study, the zero emission system reaches a high renewable share by 2050, with renewables supplying 75.7 % of total energy demand. This large share of zero MC generation drives the increase in zero-price hours. For comparison, Germany reached renewable shares of 51.4 % in electricity and 17.8 % in heat demand in 2024 [26]. In the same year, its day-ahead market recorded 459 hours with negative prices [27].

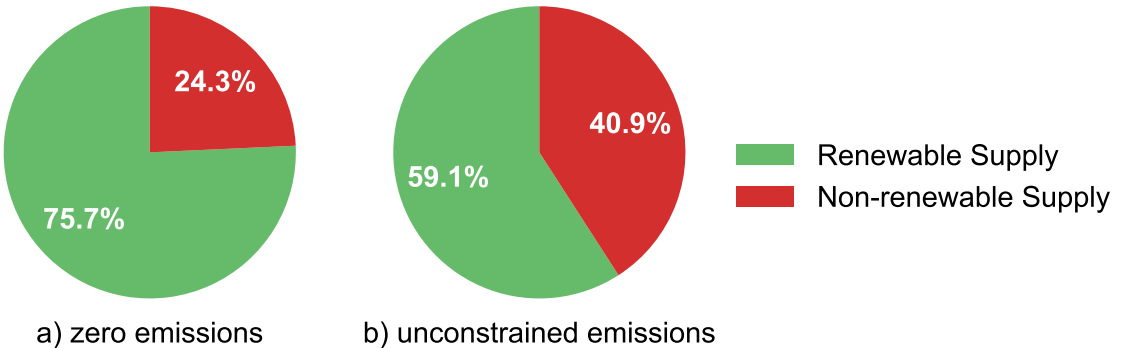


Figure 4.18.: Share of renewable energy supply in the normal-price scenario.

Figure 4.19 shows the number of peak-price electricity hours per year as a function of GWP in the normal-price scenario. Peak-prices, defined as hours above 400 € MWh^{-1} , occur only under zero emissions. As with zero-price hours, introducing demand elasticity reduces the number of peak-price hours from 612 (7.0 %) with fixed demand to 484 (5.5 %) with low elasticity and further to 323 (3.7 %) with high elasticity. Under elastic demand, consumers can decrease demand, and if this reduction deactivates all technologies with MC above the peak-price threshold, the next marginal technology sets a price below 400 € MWh^{-1} .

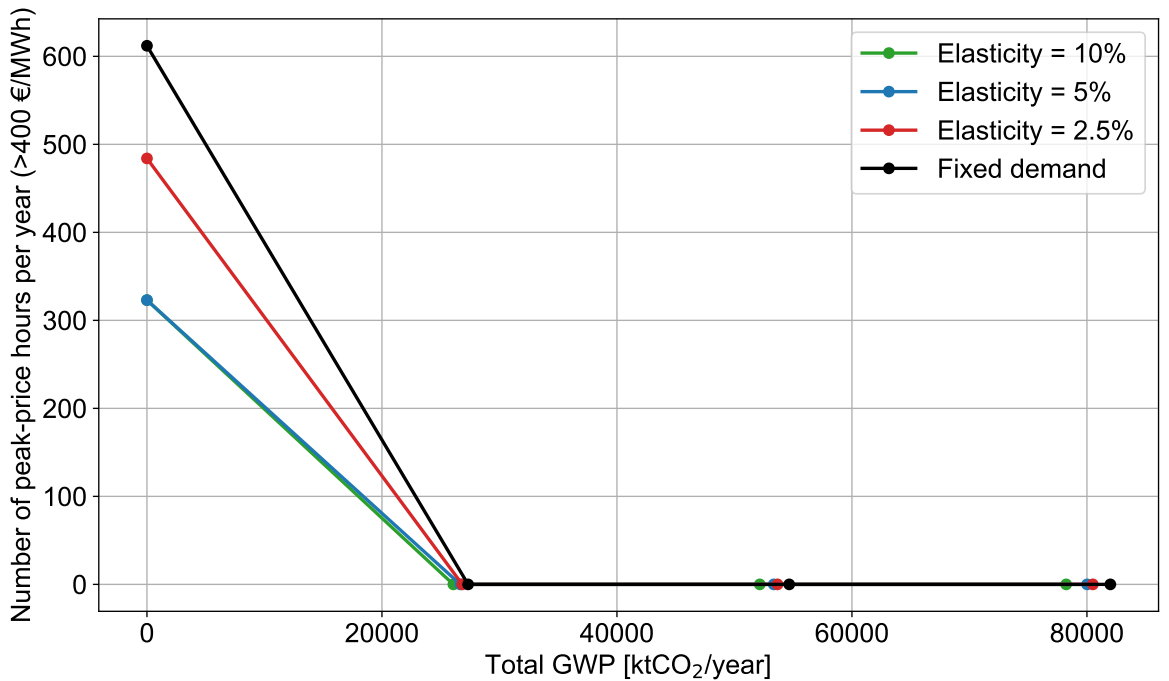


Figure 4.19.: Number of peak-price hours per year versus GWP in the normal-price scenario.

5. Conclusion and Outlook

This work integrates the spatio-temporal multi-product supply chain framework developed by the group of Prof. Zavala at the University of Wisconsin–Madison into the EnergyScope energy system model and studies stakeholder participation, demand elasticity, and price formation in a future multi-sector energy system. By reformulating EnergyScope as a coordinated market cleared by an independent system operator, the study links cost-minimizing central planner models with welfare-maximizing market formulations.

A first key contribution is the mapping of EnergyScope resources, conversion technologies, and end-use demands to profit-seeking stakeholders interacting in a spatio-temporal multi-product supply chain. Storage is integrated consistently with the typical day methodology, including seasonal storage reconstruction. Resource operating costs are represented as supply bids, while investment and fixed operation and maintenance costs remain explicitly included in the objective function. This preserves the long-term investment logic of EnergyScope while embedding it in a market clearing framework with endogenous prices.

The coordinated market relies on voluntary participation driven by economic incentives, and imposing demand destroys its key economic properties. In EnergyScope, demand is fixed, which implies that maximizing social welfare remains equivalent to minimizing total system cost. With perfectly inelastic demand, consumer bids do not influence investment or operational decisions, and the coordinated market reduces to the standard central planner outcome regardless of supply side granularity. Representing the value-of-lost-load as a market-activating bid preserves the market formulation but leads to the same result. Since electricity systems are designed to avoid unserved energy, prices rarely exceed the value-of-lost-load, no shedding occurs, and demand remains effectively fixed.

Consumers and suppliers only interact when demand is elastic. This work incorporates consumer flexibility into EnergyScope using a piecewise linear approximation of a log-log demand curve, which changes the optimization problem from a linear to a quadratic program. Solve times remain unaffected, demonstrating that demand elasticity can be included in large-scale energy system models while preserving computational efficiency.

5. Conclusion and Outlook

A case study of Germany's multi-sector energy system in 2050 shows how demand elasticity affects welfare, investment, and prices. Higher elasticity softens the trade-off between social welfare and emission reductions. Its effect on total system costs depends on the price level. At low consumer willingness to pay, higher elasticity reduces capacity expansion costs by shedding demand, while at high willingness to pay it increases consumption and investment costs. With fixed demand, system outcomes remain unchanged across price levels, highlighting that responsive consumers are necessary for meaningful price signals.

The model also provides insight into endogenous price formation. Market prices reflect both the shadow prices of nodal balance constraints and the intersection of supply and demand, where the marginal plant sets the price. Prices rise with tighter emission constraints and show characteristic temporal patterns, including midday dips driven by solar generation. Across typical days, renewable availability, sector coupling, and storage lead to different marginal stakeholders and price levels. Storage can set prices through its marginal storage value, which reflects the opportunity cost of scarcity pricing.

Flexible consumers reduce zero-price hours by increasing consumption during periods of excess renewable generation, thereby activating non-zero marginal cost plants, and mitigate peak prices by lowering demand during scarcity, which prevents the activation of high marginal cost plants. As a result, elastic demand eases price bifurcation in systems with high shares of renewable energy. These findings align with recent literature and underline the importance of demand side flexibility for price stability in future energy systems.

In conclusion, under fixed demand, no additional stakeholder competition emerges from linear market clearing formulations, such as the multi-product SC framework, compared to a cost-minimizing central planner. The value of the coordinated market perspective lies in its ability to accommodate stakeholder behavior. Introducing demand elasticity enables price–quantity interactions, allowing consumers and producers to respond to price signals and shape investment, operation, and prices in a welfare-maximizing equilibrium.

Given empirical evidence that electricity demand already exhibits non-negligible elasticity, incorporating flexible consumers is increasingly important for long-term energy system analysis. The multi-product SC EnergyScope model provides a computationally feasible and consistent framework for this purpose. Beyond demand elasticity, the framework supports future extensions, including multi-node price formation, explicit storage and transport bidding, and sector-specific consumer behavior. As such, it offers a flexible foundation for analyzing the economic dynamics of highly decarbonized and integrated energy systems.

Bibliography

- [1] Gauthier Limpens, Stefano Moret, Hervé Jeanmart, and Francois Maréchal. EnergyScope TD: A novel open-source model for regional energy systems. *Applied Energy*, 255:113729, December 2019. ISSN 0306-2619. doi: 10.1016/j.apenergy.2019.113729. URL <https://www.sciencedirect.com/science/article/pii/S0306261919314163>.
- [2] Philip A. Tominac and Victor M. Zavala. Economic properties of multi-product supply chains. *Computers & Chemical Engineering*, 145:107157, February 2021. ISSN 0098-1354. doi: 10.1016/j.compchemeng.2020.107157. URL <https://www.sciencedirect.com/science/article/pii/S0098135420305810>.
- [3] Philip A. Tominac, Weiqi Zhang, and Victor M. Zavala. Spatio-temporal economic properties of multi-product supply chains. *Computers & Chemical Engineering*, 159:107666, March 2022. ISSN 0098-1354. doi: 10.1016/j.compchemeng.2022.107666. URL <https://www.sciencedirect.com/science/article/pii/S0098135422000114>.
- [4] David Yang Shu, Christiane Reinert, Jacob Mannhardt, Ludger Leenders, Jannik Lüthje, Alexander Mitsos, and André Bardow. Overcoming the central planner approach – Bilevel optimization of the European energy transition. *iScience*, 27(7):110168, July 2024. ISSN 2589-0042. doi: 10.1016/j.isci.2024.110168. URL <https://www.sciencedirect.com/science/article/pii/S2589004224013932>.
- [5] John B. Shoven and John Whalley. Applying General Equilibrium. *Cambridge Books*, 1992. URL <https://ideas.repec.org/b/cup/cbooks/9780521266550.html>. Publisher: Cambridge University Press.
- [6] Andreas Loeschel and Christoph Boehringer. Computable General Equilibrium Models for Sustainability Impact Assessment: Status Quo and Prospects. *ECOLOGICAL ECONOMICS*, 2006. doi: 10.1016/j.ecolecon.2006.03.006. URL <https://publications.jrc.ec.europa.eu/repository/handle/JRC34342>.

Bibliography

- [7] Mingming Leng and Parlar Mahmut. Game Theoretic Applications in Supply Chain Management: A Review: *INFOR: Information Systems and Operational Research*: Vol 43, No 3, 2005. URL <https://www.tandfonline.com/doi/abs/10.1080/03155986.2005.11732725>.
- [8] Jean-Claude Hennet and Yasemin Arda. Supply chain coordination: A game-theory approach. *Engineering Applications of Artificial Intelligence*, 21(3):399–405, April 2008. ISSN 0952-1976. doi: 10.1016/j.engappai.2007.10.003. URL <https://www.sciencedirect.com/science/article/pii/S0952197607001327>.
- [9] Apoorva M. Sampat, Yicheng Hu, Mahmoud Sharara, Horacio Aguirre-Villegas, Gerardo Ruiz-Mercado, Rebecca A. Larson, and Victor M. Zavala. Coordinated management of organic waste and derived products. *Computers & Chemical Engineering*, 128:352–363, September 2019. ISSN 0098-1354. doi: 10.1016/j.compchemeng.2019.06.008. URL <https://www.sciencedirect.com/science/article/pii/S009813541930119X>.
- [10] Weiqi Zhang and Victor M. Zavala. Remunerating Space-Time, Load-Shifting Flexibility from Data Centers in Electricity Markets, August 2021. URL <http://arxiv.org/abs/2105.11416>. arXiv:2105.11416 [eess].
- [11] Tom Brown, Fabian Neumann, and legor Riepin. Price formation without fuel costs: The interaction of demand elasticity with storage bidding. *Energy Economics*, 147: 108483, June 2025. ISSN 0140-9883. doi: 10.1016/j.eneco.2025.108483. URL <https://www.sciencedirect.com/science/article/pii/S014098832500307X>.
- [12] Stefano Moret. Core version documentation - Energyscope, 2025. URL https://www.energyscope.net/main/explanation/core_version_documentation/.
- [13] Fernando Domínguez-Muñoz, José M. Cejudo-López, Antonio Carrillo-Andrés, and Manuel Gallardo-Salazar. Selection of typical demand days for CHP optimization. *Energy and Buildings*, 43(11):3036–3043, November 2011. ISSN 0378-7788. doi: 10.1016/j.enbuild.2011.07.024. URL <https://www.sciencedirect.com/science/article/pii/S037877881100329X>.
- [14] Stefano Moret and Gauthier Limpens. Typical Days - Energyscope, 2025. URL https://library.energyscope.ch/main/features/module_td/#typical-days-selection.

Bibliography

- [15] Paolo Gabrielli, Matteo Gazzani, Emanuele Martelli, and Marco Mazzotti. Corrigendum to “Optimal design of multi-energy systems with seasonal storage” [Appl. Energy (2017)]. *Applied Energy*, 212:720, February 2018. ISSN 0306-2619. doi: 10.1016/j.apenergy.2017.12.070. URL <https://www.sciencedirect.com/science/article/pii/S0306261917317853>.
- [16] T. Brown and L. Reichenberg. Decreasing market value of variable renewables can be avoided by policy action. *Energy Economics*, 100:105354, August 2021. ISSN 0140-9883. doi: 10.1016/j.eneco.2021.105354. URL <https://www.sciencedirect.com/science/article/pii/S0140988321002607>.
- [17] The CORE Team. The elasticity of demand, 2017. URL <https://books.core-econ.org/the-economy/v1/book/text/leibniz-07-08-01.html>.
- [18] Fabian Arnold. On the functional form of short-term electricity demand response - Insights from high-price years in Germany. Working Paper 23/06, EWI Working Paper, 2023. URL <https://www.econstor.eu/handle/10419/286380>.
- [19] Febin Kachirayil, David Hückebrink, Valentin Bertsch, and Russell McKenna. Trade-offs between system cost and supply security in municipal energy system design: an analysis considering spatio-temporal disparities in the Value of Lost Load. *ETH Zurich*, February 2024. URL https://ethz.ch/content/dam/ethz/special-interest/mavt/esa-dam/documents/WorkingPaperSeries/ESA_WorkingPaperSeries_No2_Final.pdf.
- [20] T. Brown, D. Schlachtberger, A. Kies, S. Schramm, and M. Greiner. Synergies of sector coupling and transmission reinforcement in a cost-optimised, highly renewable European energy system. *Energy*, 160:720–739, October 2018. ISSN 0360-5442. doi: 10.1016/j.energy.2018.06.222. URL <https://www.sciencedirect.com/science/article/pii/S036054421831288X>.
- [21] Jonas Hörsch, Fabian Hofmann, David Schlachtberger, and Tom Brown. PyPSA-Eur: An open optimisation model of the European transmission system. *Energy Strategy Reviews*, 22:207–215, November 2018. ISSN 2211-467X. doi: 10.1016/j.esr.2018.08.012. URL <https://www.sciencedirect.com/science/article/pii/S2211467X18300804>.
- [22] Climate Action Tracker. Net zero targets, 2025. URL <https://climateactiontracker.org/countries/germany/net-zero-targets/>.

Bibliography

- [23] AMPL Optimization, Inc. AMPL Optimization: Empowering Businesses and Institutions, 2025. URL <https://ampl.com/>.
- [24] Gurobi Optimization, LLC. Gurobi optimizer reference manual, 2024. URL <https://www.gurobi.com>.
- [25] Bundesnetzagentur. Bundesnetzagentur - Press - Electricity supply interruptions in 2024 shorter than in the previous year – Germany's electricity grid one of the most reliable in a European comparison, 2025. URL https://www.bundesnetzagentur.de/SharedDocs/Pressemitteilungen/EN/2025/20251009_SAIDI_Strom.html.
- [26] U. B. A. Redaktionsassistenz 1. Renewable energies in figures, June 2013. URL <https://www.umweltbundesamt.de/en/topics/climate-energy/renewable-energies/renewable-energies-in-figures>. Publisher: Umweltbundesamt.
- [27] Nora Amer, Louisa Wasmeier, Serafin von Roon, and Timo Kern. German electricity prices on EPEX Spot 2024, 2025. URL <https://www.ffe.de/en/publications/german-electricity-prices-on-epex-spot-2024/>.

A. Sets, Parameters, and Variables

This appendix documents the sets, parameters, and variables used to describe the modifications that integrate the multi-product SC framework within the core EnergyScope model, enabling the multi-product SC EnergyScope model.

A.1. Sets and Indices

• $n \in N$	Spatial nodes
• $h \in H$	Hours
• $td \in TD$	Typical days
• $t \in T$	Periods
• $i \in RES$	Resources
• $j \in TECH$	Technologies
• $eut \in EUT$	End-use types
• $s \in S \subseteq RES$	Suppliers
• $p \in P \subset TECH$	Processors
• $sto \in STO \subset TECH$	Storage technologies
• $sto_{\text{daily}} \in STO_{\text{daily}} \subset STO$	Daily storage technologies
• $inf \in INF \subset TECH$	Infrastructure technologies
• $c \in C \subseteq EUT$	Consumers
• $l \in L = RES \cup EUT$	Layers/products
• $b \in \{0, \dots, K\}$	PWL demand curve breakpoints
• $k \in \{1, \dots, K\}$	PWL demand curve segments

A.2. Parameters

A.2.1. Time Parameters

- $t_{\text{op}}^{h,td}$ Duration of hour h and typical day td pair [h]
- $w^{h,td}$ Annual weighting factor of hour h and typical day td pair [-]

A.2.2. Technology Parameters

- $\text{layers}_{\text{in,out}}^{s/j,l}$ Input/output coefficient of supplier s /technology j for layer l [-]
- τ^j Annualization factor of technology j [a^{-1}]

A.2.3. Cost Parameters

- c_{op}^s Specific operational resource costs of supplier s [$M\text{\textcent GWh}^{-1}$]
- c_{inv}^j Specific investment costs of technology j [$M\text{\textcent GW}^{-1}$]
- c_{maint}^j Specific annual fixed O&M costs of technology j [$M\text{\textcent GW}^{-1} a^{-1}$]
- VOLL Value-of-lost-load [$M\text{\textcent GWh}^{-1}$]

A.2.4. Demand Parameters

- $\text{End}_{\text{uses}}^{c,h,td}$ End-use demand [GW]
- $d_{\text{ref}}^{c,n,h,td}$ Reference demand [GW]
- $p_{\text{ref}}^{c,n,h,td}$ Reference price [$M\text{\textcent GWh}^{-1}$]
- ϵ Price elasticity of demand [-]
- $\beta^{c,n,h,td}$ Log-log demand curve exponent [-]
- $A^{c,n,h,td}$ Log-log demand curve parameter
- d_{fix} Binary flag for fixed demand [-]

A.2.5. Piecewise Linear Demand Parameters

• d_{mult}^b	Demand multiplier at breakpoint b [—]
• $d_{\text{pwl}}^{b,c,n,h,td}$	Demand at breakpoint b [GW]
• $p_{\text{pwl}}^{b,c,n,h,td}$	Price at breakpoint b [M€ GWh $^{-1}$]
• $D^{k,c,n,h,td}$	Width of demand segment k [GW]
• $a^{k,c,n,h,td}$	Intercept of demand segment k [M€ GWh $^{-1}$]
• $b^{k,c,n,h,td}$	Slope of demand segment k [M€ GWh $^{-2}$]

A.3. Decision Variables

A.3.1. Independent Variables

• $g^{s,n,h,td}$	Supplier s flow [GW]
• F^j	Installed capacity of technology j [GW, storage GWh]
• $e^{p,n,h,td}$	Processor p flow [GW]
• $\text{Storage}_{\text{in}}^{sto,l,n,h,td}$	Storage sto charging power [GW]
• $\text{Storage}_{\text{out}}^{sto,l,n,h,td}$	Storage sto discharging power [GW]
• $d^{c,n,h,td}$	Consumer c flow [GW]

A.3.2. Dependent Variables

• $\text{Storage}_{\text{level}}^{sto,n,t}$	Storage sto state of charge [GWh]
• $\text{Storage}_{\text{level,daily}}^{sto_{\text{daily}},n,h,td}$	Daily storage sto_{daily} state of charge [GWh]
• $d_{\text{diff}}^{c,n,h,td}$	Difference between actual and reference demand [GW]
• $d_{\text{seg}}^{k,c,n,h,td}$	Demand in segment k [GW]
• C_{op}^i	Annual operating costs of resource i [M€ a $^{-1}$]
• C_{inv}^j	Annualized investment costs of technology j [M€ a $^{-1}$]
• C_{maint}^j	Annual fixed O&M costs of technology j [M€ a $^{-1}$]

A.3.3. Dual Variables

- $\pi^{eut,h,td}$ Balance constraint dual variable for end-use eut [€MWh^{-1}]
- π_{eut}^{eut} Yearly average price for end-use eut [€MWh^{-1}]

A.4. Objective Variables

- TotalCost Total system cost [M€ a^{-1}]
- SocialWelfare Social welfare [M€ a^{-1}]

B. Flows

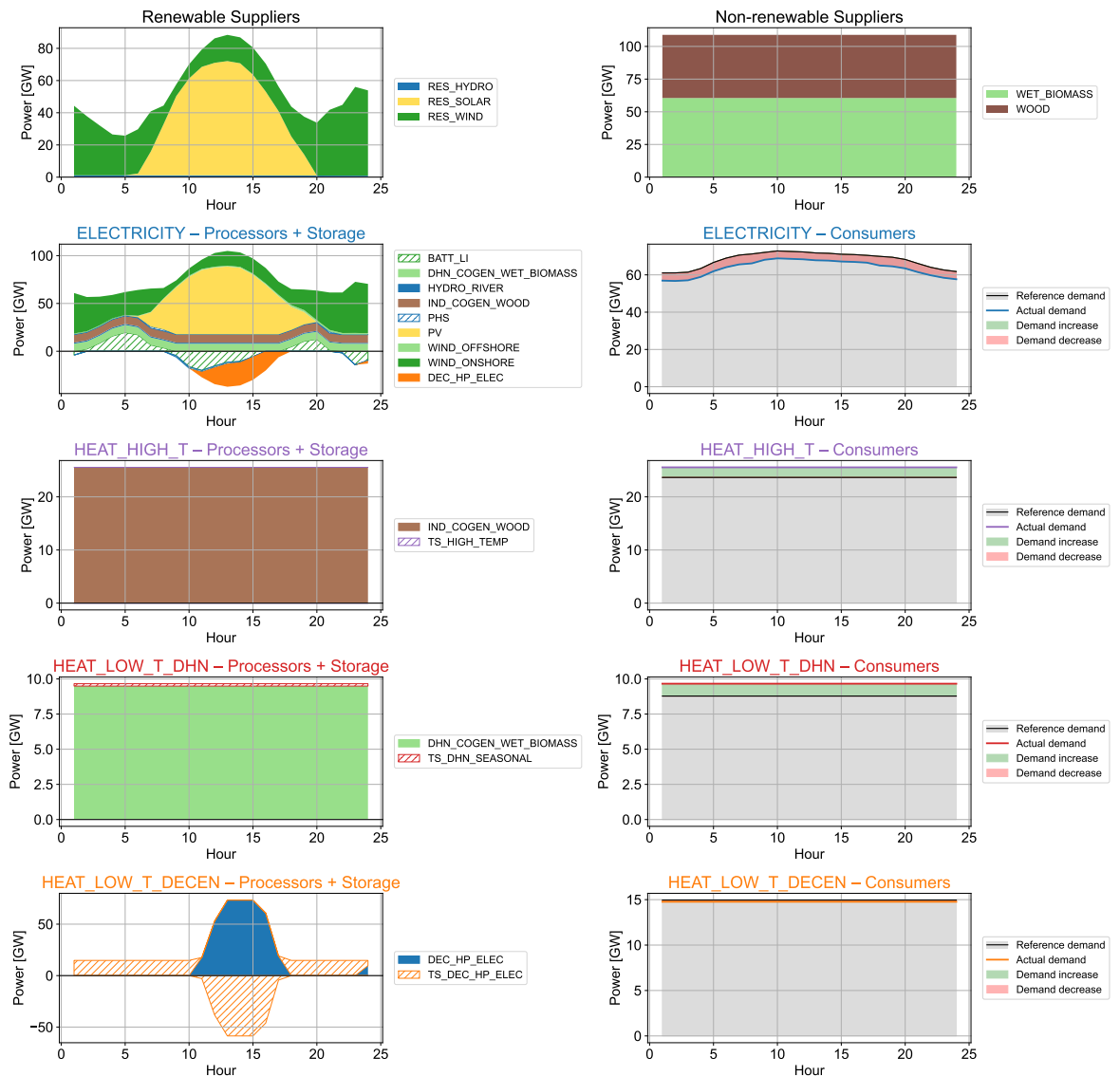


Figure B.1.: Stakeholder flow on TD 9 for the normal-price zero-emission scenario.

B. Flows

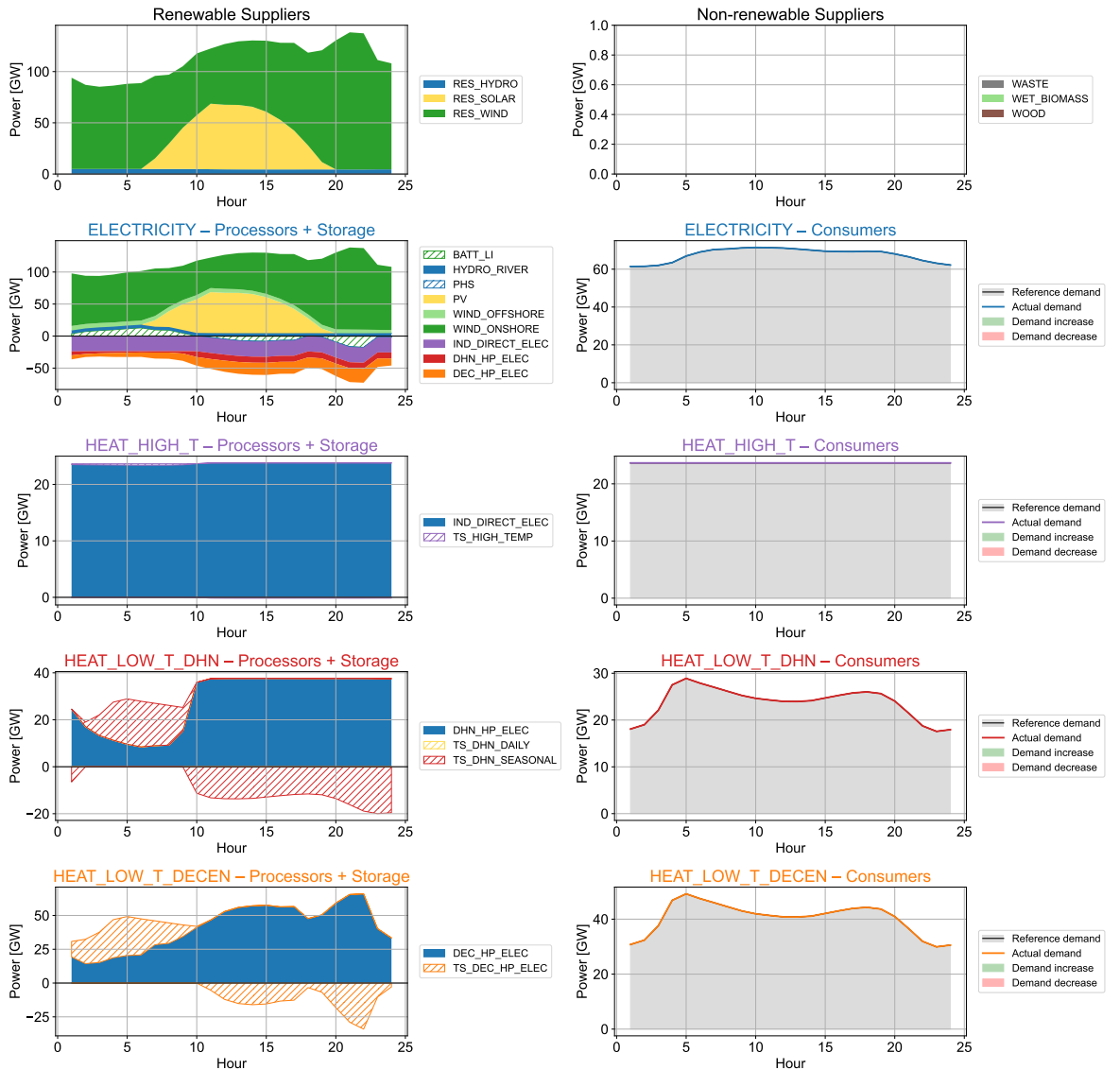


Figure B.2.: Stakeholder flow with fixed demand on TD 4 for the normal-price zero-emission scenario.

B. Flows

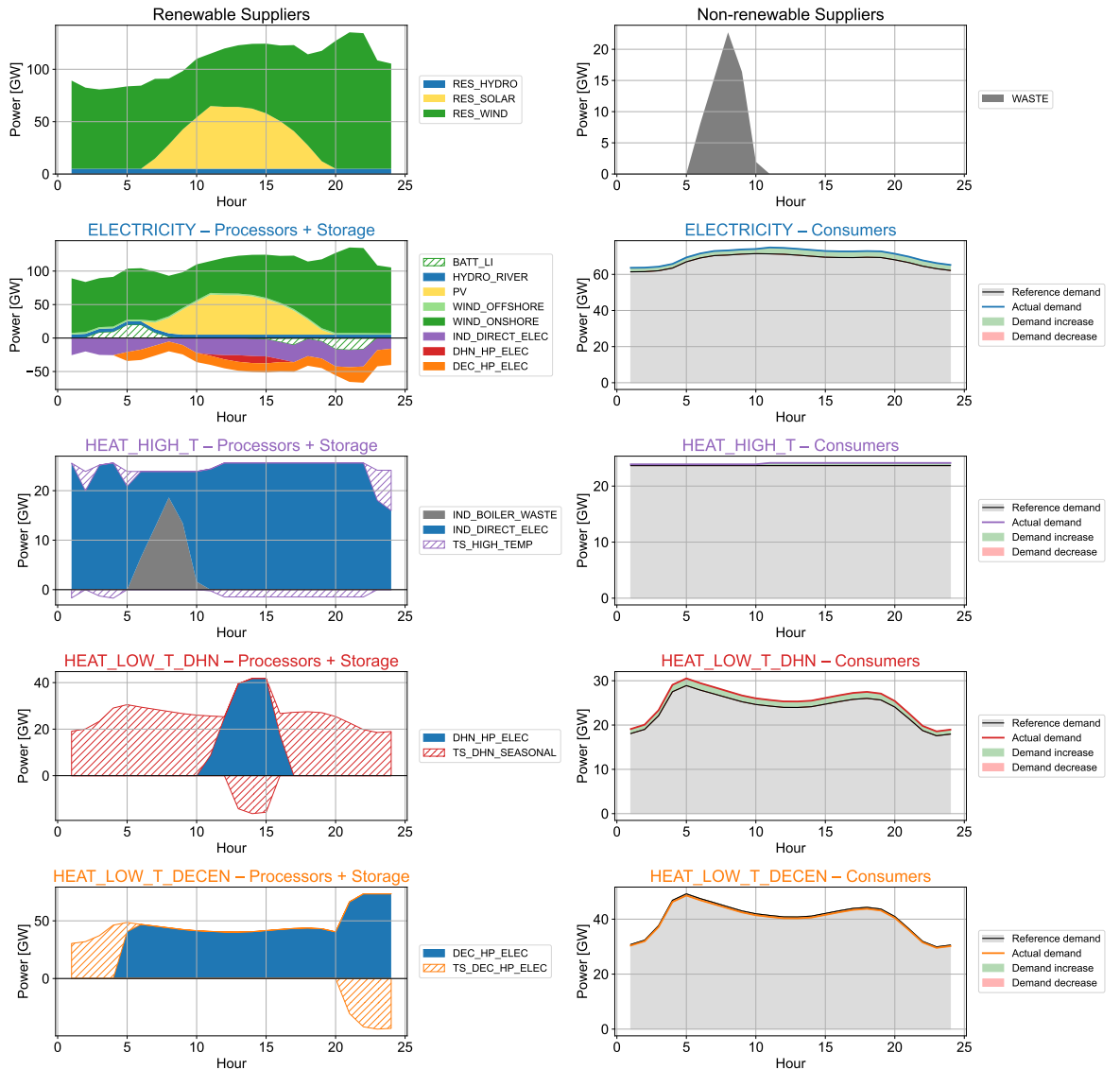


Figure B.3.: Stakeholder flow with 5% elasticity on TD 4 for the normal-price zero-emission scenario.

B. Flows

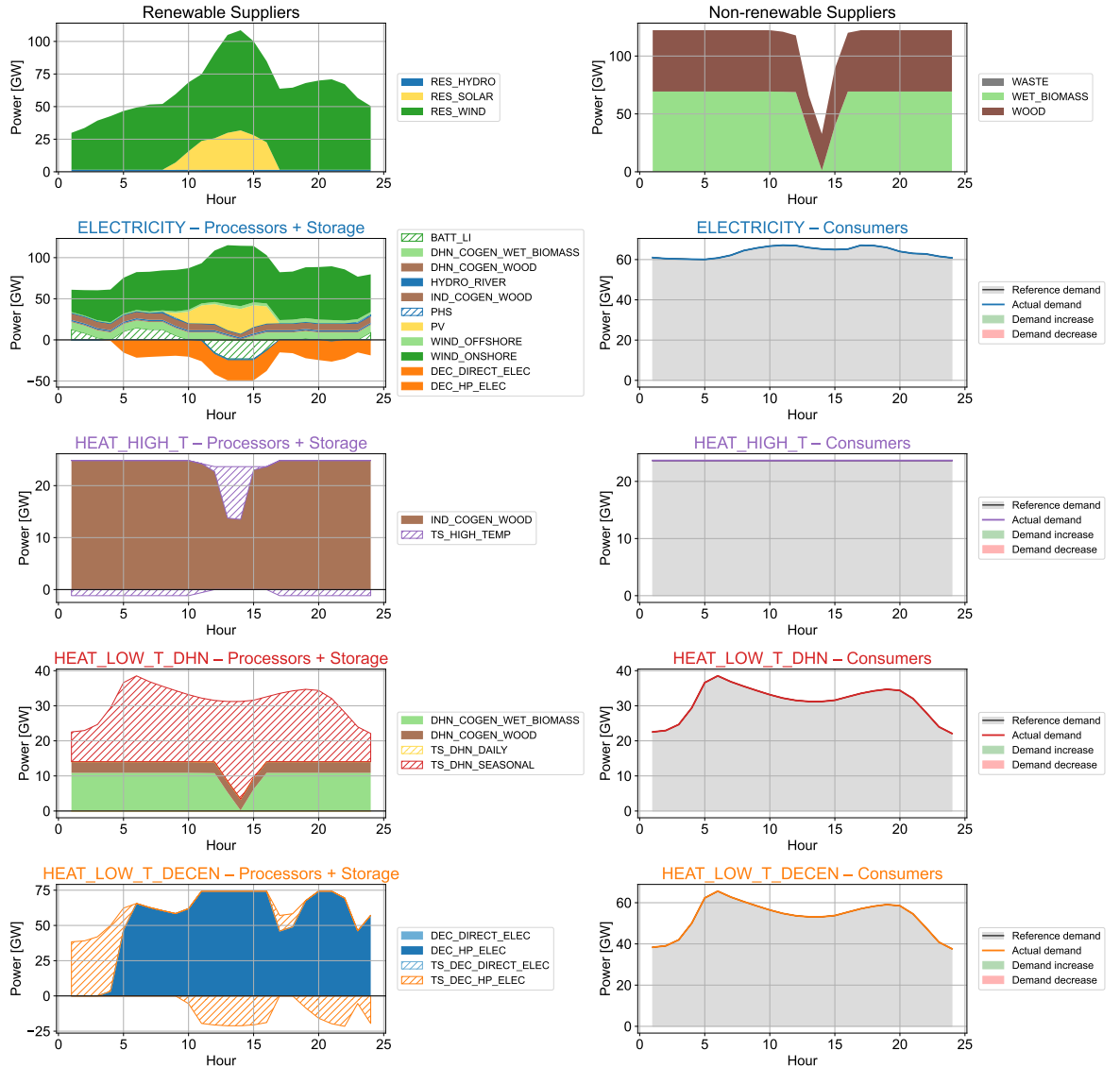


Figure B.4.: Stakeholder flow with fixed demand on TD 11 for the normal-price zero-emission scenario.

B. Flows

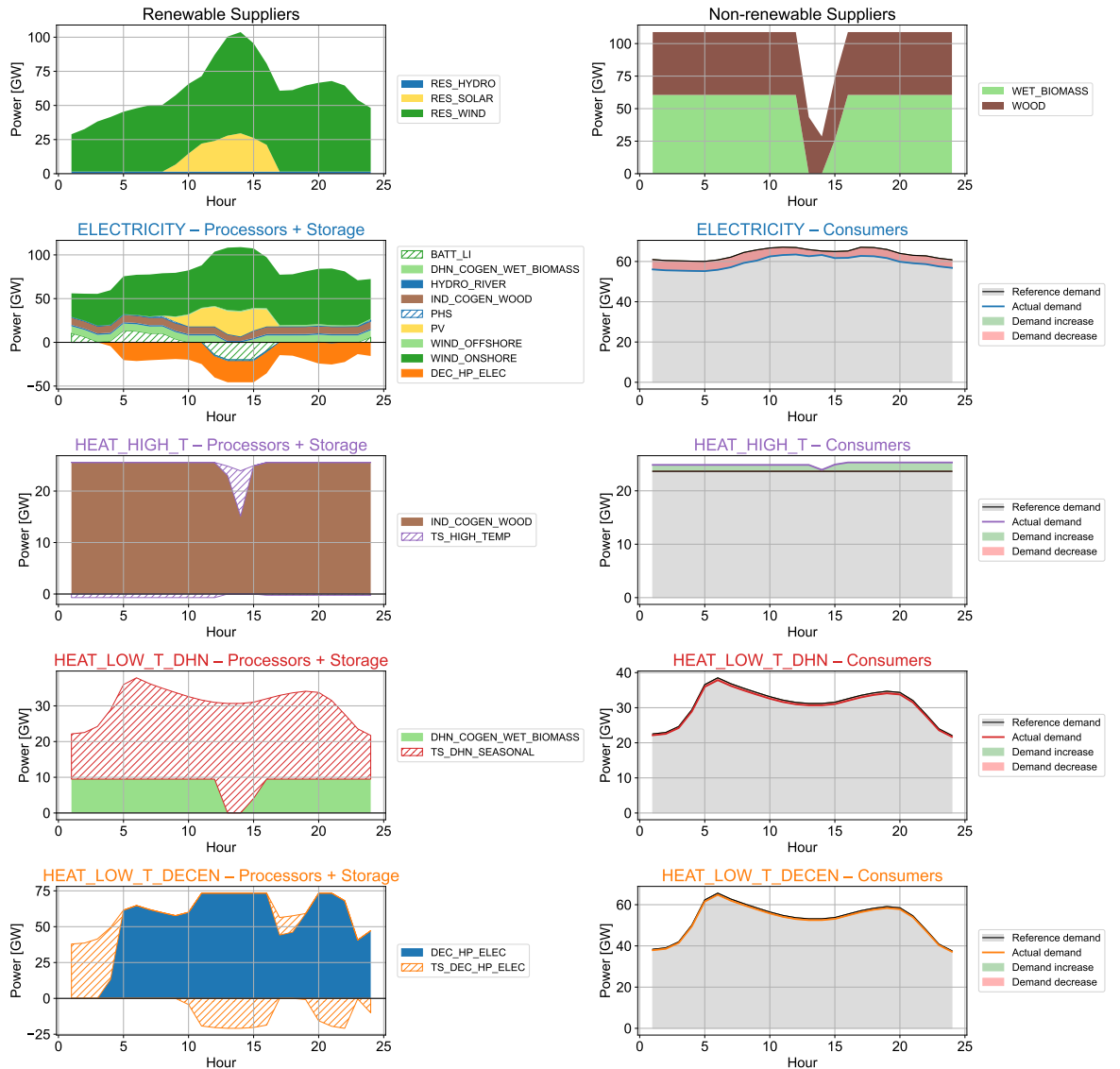


Figure B.5.: Stakeholder flow with 5% elasticity on TD 11 for the normal-price zero-emission scenario.

Eigenständigkeitserklärung

Die unterzeichnete Eigenständigkeitserklärung ist Bestandteil jeder während des Studiums verfassten schriftlichen Arbeit. Eine der folgenden zwei Optionen ist **in Absprache mit der verantwortlichen Betreuungsperson** verbindlich auszuwählen:

- Ich erkläre hiermit, dass ich die vorliegende Arbeit eigenverantwortlich verfasst habe, namentlich, dass mir niemand beim Verfassen der Arbeit geholfen hat. Davon ausgenommen sind sprachliche und inhaltliche Korrekturvorschläge der Betreuungsperson. Es wurden keine Technologien der generativen künstlichen Intelligenz¹ verwendet.
- Ich erkläre hiermit, dass ich die vorliegende Arbeit eigenverantwortlich verfasst habe. Dabei habe ich nur die erlaubten Hilfsmittel verwendet, darunter sprachliche und inhaltliche Korrekturvorschläge der Betreuungsperson sowie Technologien der generativen künstlichen Intelligenz. Deren Einsatz und Kennzeichnung ist mit der Betreuungsperson abgesprochen.

Titel der Arbeit:

Multi-product Supply Chain Optimization for Energy Systems

Verfasst von:

Bei Gruppenarbeiten sind die Namen aller Verfasserinnen und Verfasser erforderlich.

Name(n):

Pielmaier

Vorname(n):

Konstantin

Ich bestätige mit meiner Unterschrift:

- Ich habe mich an die Regeln des «[Zitierleitfadens](#)» gehalten.
- Ich habe alle Methoden, Daten und Arbeitsabläufe wahrheitsgetreu und vollständig dokumentiert.
- Ich habe alle Personen erwähnt, welche die Arbeit wesentlich unterstützt haben.

Ich nehme zur Kenntnis, dass die Arbeit mit elektronischen Hilfsmitteln auf Eigenständigkeit überprüft werden kann.

Ort, Datum

Zürich, 21.12.2025

Unterschrift(en)

Bei Gruppenarbeiten sind die Namen aller Verfasserinnen und Verfasser erforderlich. Durch die Unterschriften bürgen sie grundsätzlich gemeinsam für den gesamten Inhalt dieser schriftlichen Arbeit.

¹ Für weitere Informationen konsultieren Sie bitte die Webseiten der ETH Zürich, bspw. <https://ethz.ch/de/die-eth-zuerich/lehre/ai-in-education.html> und <https://library.ethz.ch/forschen-und-publizieren/Wissenschaftliches-Schreiben-an-der-ETH-Zuerich.html> (Änderungen vorbehalten).